Mineralogy and petrography of technogenic parabasalts from the Chelyabinsk brown coal basin

Article *in* Geologiya i Geofizika · June 1999

CITATIONS
26

READS
90

6 authors, including:

Victor Victorovich Sharygin
Sobolev Institute of Geology and Mineralogy
280 PUBLICATIONS **2,075** CITATIONS
SEE PROFILE

Ella Sokol
Sobolev Institute of Geology and Mineralogy
121 PUBLICATIONS **1,273** CITATIONS
SEE PROFILE

V. M. Kalugin
Sobolev Institute of Geology and Mineralogy
12 PUBLICATIONS **270** CITATIONS
SEE PROFILE

Russian Geology and Geophysics
Vol. 40, No. 6, pp. 879-899, 1999

Geologiya i Geofizika
UDC 549.01

MINERALOGY AND PETROGRAPHY OF TECHNOGENIC PARABASALTS FROM THE CHELYABINSK BROWN-COAL BASIN

V. V. Sharygin, E. V. Sokol, E. N. Nigmatulina, G. G. Lepezin, V. M. Kalugin, and A. E. Frenkel'

United Institute of Geology, Geophysics and Mineralogy, Siberian Branch of the RAS, prosp. Akad. Koptyuga 3, Novosibirsk, 630090, Russia

Spontaneous burning in the largest spoil heaps of the Chelyabinsk coal basin initiated high-temperature conditions (1000–1300 °C). At these parameters, Fe-rich basic liquids resulted from the complete melting of a finely crushed mixture of mudstones, calcareous clays, and siderites in zones of heaps with reductive gas annealing. Crystallization of these melts under dry reductive conditions ($f_{O_2} = 10^{-9}-10^{-12}$, T = 1200–1000 °C) at pressure close to 1 atm led to formation of parabasalts. These rocks differ greatly from all natural paralavas and terrestrial basalts in having high Al_2O_3, FeO, CaO, P_2O_5 and low SiO_2, MgO, Fe_2O_3, and Na_2O contents. Plagioclase (An_{100-90}), Mg-Fe-clinopyroxene (diopside, low- and high-alumina augite), and Mg-Fe-olivine (Fo_{60-15}) are the main rock-forming minerals in the parabasalts. Fayalite (Fo_{10-3}), Ti-magnetite, Al-spinel, leucite, hedenbergite, kirschsteinite, pyrrhotite, K-feldspar, fluorapatite, ilmenite, and glasses of two compositions (K-acidic and Fe-basic) are minor phases. Low-Ca pyroxenes (orthopyroxene, pigeonite), tridymite and other SiO_2 polymorphs, mullite, nepheline, chalcopyrite, pyrite, native iron, and shungite are found as accessories. Some minerals contain uncommon admixtures. Olivines contain up to 15 mol.% larnite end-member, some olivines and kirschsteinites have P_2O_5 (up to 0.7 wt.%), apatite is rich in SiO_2 (up to 6 wt.%), and K-feldspar is rich in BaO (up to 7.5 wt.%). In textural features, modal composition, mineral ratios, and order of mineral crystallization, the technogenic parabasalts correspond to shallow-depth basic rocks.

Clinopyroxene, fayalite, kirschsteinite, leucite, pyrrhotite, paralava, basalt, spoil heap, Chelyabinsk coal basin

INTRODUCTION

Underground fires of coal deposits are known in almost all coal basins of the world. Resulting high-temperature processes cause intense annealing, slagging, and baking of sedimentary rocks, forming complexes of fused rocks. In spite of very high temperatures, occasionally to 1000 °C, melting processes are poorly developed in these objects and, as a rule, are limited to local formation of eutectoid melts (T = 900–1100 °C) of a wide range of compositions. The most abundant rocks are buchites – fritted rocks, which are highly heterogeneous and contain considerable amounts of glass [1–4]. An example is fritted Ca-bearing mudstones of Buffalo (Wyoming, USA) [4]. On slagging of clay slates and diatomites of California at 1100 °C, dry granite eutectics partially melted, whereas the complete melting of the rocks of this complex was achieved at 1600 °C [5]. Melting processes are widely developed at the Kenderlyk occurrence of iron-ore paralavas in Eastern Kazakhstan [6]. The source of melt was a mixture of carbonate-clay sediments and siderites. The reducing gas medium provided mobilization of appreciable amounts of iron into silicate melts and favored rather low-temperature (T = 900–1100 °C) conditions of their formation. Crystallization occurred at increasing oxygen potential, which resulted in ore basalts similar to magmatogene ones.

The object of our studies is technogenic basic paralavas – products of melting of waste mass in the heaps of the Chelyabinsk coal basin and further crystallization of the melts in hot spoil heaps. Fused rocks have been found only in the largest and intensely burned spoil heaps of the Korkinskii opencasting and coal mines no. 42 and Komsomol'skaya in Kopeisk. They were for the first time described by Chesnokov and

Shcherbakova [7], and the more detailed description of their mineralogy and petrography is reported in [8–10]. We named technogenic basic paralavas parabasalts, because this term best of all reflects both the initial sedimentary nature of melted substance and its final mineral composition.

Technogenic parabasalts of the Southern Urals have an extremely unusual chemical composition (wt.%): SiO_2 = 37.8–50.1; Al_2O_3 = 14.5–18.9; CaO = 10.5–16.4; FeO = 11.9–20.3; MgO = 3.4–6.5; Na_2O < 0.3; K_2O = 0.8–2.1 [8, 9]. These parabasalts and flood basalts containing native iron have some similar features [11]. Xenoliths of olivine gabbros and gabbronorites in basalts of the Kuril-Kamchatka belt and lunar low- and moderate-magnesium basalts and dolerites [12–14] appeared to be the most similar to the rocks which we have studied. The presence of leucite and Ba-feldspar in these rocks suggests their similarity to some alkali basalts, in particular, to leucite-bearing lavas of Italy (Vesuvius, Roman province) [15–17]. Among technogenic products, close analogs are slags and iron-ore agglomerates synthesized under reductive conditions [10].

The parabasalts from the Southern Urals differ from all earlier described groups of paralavas in unusual chemical and mineral compositions, individual features of minerals, minor amount of glass, large (to 1.5 mm) crystal sizes, and texture and structure corresponding to those of natural dolerites. This permits them to be treated as a new type of exogenic melts. The aim of this paper is to describe mineralogy and petrography of parabasalts and to reconstruct generation conditions for their initial melting.

MINERALOGIC AND PETROGRAPHIC DESCRIPTION OF PARABASALTS

Technogenic parabasalts from spoil heaps of the Chelyabinsk coal basin may be divided into three morphologic varieties (Table 1): *massive parabasalt, parabasalt dropstone, and veined parabasalt*.

Massive parabasalts were found at the bottom of the spoil heap in the Korkinskii opencasting [7, 18]. Blocks of these rocks are very similar to basalts, reach a few cubic meters in size, and are an aggregate of fritted rocks and a considerable (to 50 vol.%) amount of large fragments of annealed mudstones. According to Chesnokov [7, 18], the initial melt flowing into contraction fractures of waste mass formed 0.5–1 m thick dikes and cemented cavities between lumps of fused rocks.

Massive parabasalts (samples KR-5 and KR-6) are massive fine-grained, holocrystalline grayish-green rocks. Their texture is similar to the dolerite one. Small cavities contain crystals of clinopyroxene olivine, leucite, plagioclase, and needles of mullite. Mineral composition is fairly constant: Mg-Fe-clinopyroxene, Ca-rich plagioclase, Mg-Fe-olivine, Al-spinel, and leucite. The interstices are filled with Ti-magnetite, fayalite, pyrrhotite, K-feldspar, and (very seldom) finely devitrified opaque glass.

Parabasalt dripstone is a rare morphologic type combining stalactites, stalagmites, and drop-shaped rocks formed by iron-silicate melts flowing down to the bottom of the heap. The studied sample (stalagmite – sample 0107) was picked up by B. V. Chesnokov from the cavity in the lower part of the spoil heap of the Korkinskii opencasting. It exhibits a typical texture of flowing melt in its viscous plastic state. The rock is dark-brown and consists of plagioclase, clinopyroxene, zonal spinel (center is Al-spinel, periphery is titanomagnetite), Fe-olivine, leucite, and finely devitrified opaque glass. Interstices are filled with titanomagnetite and pyrrhotite, of lesser occurrence is kirschsteinite. A characteristic feature is skeletal olivine and leucite crystals and "stellate" segregations of Al-spinel in plagioclase and clinopyroxene, which suggests their rapid quenching. Similar morphologic features are common to minerals from the paralavas of Wyoming [3, 4].

Veined parabasalts were found among blocks of annealed surrounding rocks near the bottom of the spoil heaps of mines no. 42 and Komsomol'skaya (samples 42-17 and 063-45, respectively). They are very similar to basalts and fill interstices between fragments of annealed mudstones and carbonate rocks. Veinlets have an intricate branch-like arrangement in sinter mass, and their thickness is no more than 2–3 cm. Typical zoning occurs as a change in color, mineral composition, and granularity of rocks. Peripheral zones are microcrystalline and correspond in mineral composition to massive parabasalts. In the center of veinlets the crystals attain 0.5–1 mm in size, and in small cavities – 1.5 mm. Clinopyroxene, spinellide, and olivine from the central zone exhibit optical and chemical zoning. Interstices are filled with leucite, titanomagnetite, fayalite, hedenbergite, pyrrhotite, kirschsteinite, apatite, K-Ba-feldspar, K-acidic glass, and, less often, ilmenite. In general, the central zones of these rocks are specific "pegmatoid formations", corresponding in mineral composition to interstitial association of massive parabasalts.

Noteworthy are reactional mineral associations formed at the contacts of veined parabasalts with sedimentary rocks. At the boundary with annealed mudstones they display fine-grained chilled zones (to 0.5 cm) consisting of K-bearing cordierite, acidic K-Al-glass, and ilmenite (±rutile). When approaching parabasalt, first Al-spinel (±magnetite) and then plagioclase appear in these zones. At the contact with high-alumina

Table 1

Chemical and Mineral Compositions of Technogenic Parabasalts of the Southern Urals

Component	Morphologic type				
	parabasalt dropstone	massive parabasalt		veined parabasalt	
	Sample 0107	Sample KR	Sample KR-5	Sample 42-17-1	Sample 42-17-2
SiO_2, wt.%	37.78	45.65	44.06	43.32	50.07
TiO_2	0.94	1.07	0.93	0.73	0.94
Al_2O_3	14.46	17.97	17.26	16.29	18.88
Fe_2O_3	1.57	1.19	0.94	1.41	0.92
FeO	18.82	12.64	11.29	16.92	11.03
MnO	0.26	0.27	0.21	0.24	0.19
MgO	5.61	4.62	5.67	6.46	3.38
CaO	16.07	13.86	16.39	11.53	10.53
Na_2O	0.17	0.20	0.05	0.24	0.33
K_2O	1.46	1.37	1.48	0.77	2.09
P_2O_5	0.77	0.68	0.51	0.36	0.41
F	0.09			0.02	
S	0.10			0.04	
CO_2	0.62			0.45	
Total	98.72	99.46	98.79	98.64	98.77
Cr, ppm	140			120	
V	170			180	
Ni	40			61	
Co	1.4			1.0	
Nb	11			5	
Y	60			36	
Sc	22			13	
Th	18			16	
Li	26			11	
Rb	50			20	
Cs	3			2	
Minerals, vol.%	Sample 0107	Samples KR-5 and KR-6		Samples 42-17 and 063-45	
Al-spinel	3–5	1–2		1–2	
Anorthite	45–50	45–50		40–50	
Mg-Fe-clinopyroxene	30–40	35–45		30–40	
Mg-Fe-olivine	0.5–1	2–3		2–3	
Leucite	1–2	2–3		3–5	
Titanomagnetite	5–7	7–10		7–10	
Apatite	< 0.5	< 0.5		1–2	
Pyrrhotite	0.5–1	3–4		3–4	
Fayalite	2–3	1–2		2–3	
Kirschsteinite	< 0.5	–		1–2	
Hedenbergite	–	< 0.5		5–10	
Fe-basic glass	5–10	< 0.5		< 0.5	
K-Ba-feldspar	–	1–2		1–2	
Ilmenite	–	–		< 0.5	
K-acidic glass	–	< 0.5		1–2	

Note. Chemical analysis of sample KR is taken from [7]. Samples 42-17-1 and 42-17-2 are central and peripheral zones of veined parabasalts, respectively. F, CO_2, S, and trace elements were determined at the Institute of Geochemistry, Irkutsk.

rocks, which initially contained kaolinite and diaspore, an association corundum + SiO_2 + cordierite ± acidic glass was identified. A clear mineralogic zoning is observed at the boundary with a fragment of roasted petrified wood of dolomite-ankerite composition. The core of this xenolith is composed of fine-grained aggregates of oldhamite, CaS; ferropericlase, (Mg,Fe)O; portlandite, $Ca(OH)_2$ (initially CaO); and chlormayenite, $Ca_{13}Al_{14}(SiO_4)_{0.5}O_{32}Cl_2$. In the next zone (toward parabasalt), magnesioferrite, P-bearing larnite, and gehlenite appear in this mass. At the immediate contact with parabasalt coarse-grained low-alumina melilite is present. Somewhat different zoning is typical of the contact with siderites: magnesioferrite + Ca-rich ferrites + periclase; periclase + melilite; melilite; parabasalt.

CHEMICAL COMPOSITION OF PARABASALT MINERALS

In parabasalts of the Southern Urals the major rock-forming minerals are plagioclase and clinopyroxene; the minor phases consist of olivine, magnetite, Al-spinel, leucite, K-feldspar, sulfides, kirschsteinite, apatite, and glass (see Table 1).

Plagioclase in all types of parabasalts is close to anorthite (Table 2). The content of Na_2O usually does not exceed 0.3 wt.%, increasing to 0.6–1.3 wt.% in veined parabasalts only at the immediate contact of crystals with acidic glass or K-feldspar. The amount of K_2O varies from 0.2 to 3 wt.%, and BaO content amounts to 0.7 wt.%. Some individual grains in the dropstone and massive parabasalts contain FeO (to 1.5 wt.%) and MgO (to 0.3 wt.%). In general, plagioclase evolves with a slight increase in orthoclase and albite components. Most grains are polysynthetic twins, some display optical zoning, some contain crystallites of dark-green spinel (Fig. 1, *a*); of scarce occurrence are single crystallites of clinopyroxene, magnetite, and leucite.

Clinopyroxene in parabasalts is the main mafic mineral. It forms euhedral grains 0.05 to 0.5 mm in size. Three groups of compositions (by nomenclature proposed by the IMA [19]) are predominant: diopside-hedenbergites, low- and high-alumina augites, and pigeonite. Each variety of parabasalts contains clinopyroxenes of particular composition (Table 3). Massive rocks are dominated by diopsides (Mg# = Mg/(Mg + Fe) – 0.6–0.76) containing Al_2O_3 (2–6 wt.%) and TiO_2 (0.5–1.1 wt.%) and exhibiting well-pronounced zoning. In crystals, the concentrations of MgO and SiO_2 decrease and those of FeO, Al_2O_3, and TiO_2 increase from core to rim. Dropstone clinopyroxenes belong to high-alumina augites (Mg# – 0.44–0.57) and display a decrease in concentrations of Al_2O_3, MgO, and TiO_2 and an increase in SiO_2, FeO, and MnO contents from core to rim. Veined parabasalts contain a great diversity of clinopyroxenes (low-alumina augite, high-alumina augite, and hedenbergite), the majority of them belong in composition to the first two types. The contents of components in these minerals vary as follows (wt.%): Al_2O_3 from 1 to 16, SiO_2 – from 40 to 51, MgO – from 0.5 to 12, FeO – from 6 to 26 wt.%. In addition to chemical inhomogeneity, there is a well-observed optical zoning: a pink center (augite) and dark-green rim (hedenbergite). The compositions of clinopyroxenes from the central zones of veined parabasalts change toward higher contents of FeO and MnO and lower concentrations of MgO, TiO_2, and Al_2O_3 at approximately constant amounts of SiO_2 and CaO. Thus, during the crystallization of veined parabasalt, clinopyroxenes evolved from low-alumina augite through high-alumina augite to virtually pure hedenbergite.

In addition to high-calcium clinopyroxenes in veined parabasalts, localized near the contact with annealed mudstones, there also exist pyroxenes with low concentrations of CaO and Al_2O_3 and fairly high contents of MnO (0.4–0.8 wt.%). According to content of CaO, they are divided into three groups (Table 4). The first (CaO < 2.3 wt.%) can be conventionally referred to enstatites (Mg# – 0.52–0.67) and ferrosilites (by IMA's nomenclature [19]). Since their X-ray identification involved difficulties, we do not rule out the presence of clinoenstatites (clinoferrosilites) in the rocks. The orthorhombic and monoclinic phases of similar compositions were earlier found by Chesnokov and Shcherbakova [7]. The second group of low-calcium pyroxenes corresponds to pigeonites (CaO – 5.5–6.5 wt.%, Mg# – 0.42–0.53), and the third – to subcalcium augites (CaO – 10.9–15.6 wt.%, Mg# – 0.34–0.62).

Olivine is represented by two generations. The early generation (it includes the majority of grains) is fairly large (to 0.5–1 mm) crystals of hortonolites–ferrohortonolites (f = Fe/(Fe + Mg) = 44–84%), and the late generation is single small (< 100 μm) oval and xenomorphic grains in interstices. The crystals of this generation correspond to nearly pure fayalite (f = 86–95%) (Table 5, Fig. 2). All olivines are zonal with respect to Fe, Mg, Mn, and Ca. The maximum contents of MnO, CaO, and P_2O_5 are 2.9, 7.5, and 0.7 wt.%, respectively. The contents of chromium and nickel are at detection limit. Olivines from massive parabasalts have the lowest concentrations of CaO (to 1.4 wt.%), olivines from dropstones contain to 2.3–3.7 wt.% CaO. In minerals from veined parabasalts the content of CaO varies from 0.02 to 7.5 wt.%, with maximum

Table 2

Chemical Composition (wt.%) of Plagioclases from Parabasalts of the Southern Urals

Component	Parabasalt dripstone						Massive parabasalt						Veined parabasalt						
	Sample 0107						Sample KR-5			Sample KR-6			Sample 42-17						Sample 063-45
	core	rim	core	rim			core	rim			core	rim		core	rim		core*	rim*	
SiO_2	44.57	45.12	44.60	45.03	46.44	47.03	44.93	44.43	48.01	44.40	43.73	43.71	43.93	43.63	44.82	44.46	46.06	46.21	45.25
TiO_2	0.03	0.03	0.04	0.02	0.02	0.03	0.02	0.00	0.05	0.00	0.00	0.01	0.01	0.02	0.02	0.00	0.01	0.00	0.01
Al_2O_3	33.96	33.18	33.91	33.32	32.80	31.64	34.92	34.75	31.26	35.39	34.45	34.35	35.30	35.18	34.02	34.67	33.37	33.39	34.01
FeO	1.17	1.31	1.11	1.35	1.07	1.27	0.68	0.75	0.80	0.81	1.31	0.91	0.26	0.38	0.91	0.84	0.52	0.63	0.61
MnO	0.00	0.01	0.03	0.03	0.00	0.03	0.03	0.02	0.04	0.02	0.04	0.02	0.00	0.00	0.00	0.03	0.01	0.04	0.04
MgO	0.22	0.27	0.25	0.27	0.14	0.14	0.12	0.08	0.08	0.13	0.15	0.11	0.04	0.08	0.09	0.06	0.08	0.05	0.05
CaO	19.12	18.66	19.20	18.86	17.23	16.32	19.43	19.03	15.24	19.25	19.42	19.46	20.01	19.79	19.19	19.36	18.12	18.01	18.45
BaO	0.00	0.01	0.04	0.08	0.16	0.29	0.00	0.04	0.13	0.00	0.02	0.00	0.03	0.00	0.00	0.03	0.00	0.00	0.02
Na_2O	0.20	0.28	0.31	0.49	0.53	0.45	0.26	0.30	0.66	0.21	0.25	0.31	0.08	0.20	0.45	0.27	1.26	1.34	0.81
K_2O	0.37	0.65	0.37	0.53	1.45	2.01	0.29	0.31	3.05	0.22	0.28	0.40	0.12	0.19	0.31	0.20	0.21	0.19	0.23
Total	99.64	99.51	99.84	99.98	99.84	99.21	100.67	99.70	99.32	100.44	99.66	99.28	99.79	99.47	99.81	99.93	99.64	99.87	99.47
Total formula calculated for 8 oxygens																			
Si	2.080	2.109	2.079	2.099	2.160	2.205	2.070	2.067	2.244	2.050	2.046	2.051	2.041	2.036	2.086	2.066	2.136	2.139	2.105
Ti	0.001	0.001	0.001	0.001	0.001	0.001	0.001	0.000	0.002	0.000	0.000	0.000	0.000	0.001	0.001	0.000	0.000	0.000	0.000
Al	1.868	1.828	1.863	1.831	1.799	1.748	1.896	1.906	1.722	1.926	1.900	1.900	1.933	1.935	1.866	1.899	1.824	1.822	1.865
Fe^{2+}	0.046	0.051	0.043	0.053	0.042	0.050	0.026	0.029	0.031	0.031	0.051	0.036	0.010	0.015	0.035	0.033	0.020	0.025	0.024
Mn	0.000	0.000	0.001	0.001	0.000	0.001	0.001	0.001	0.002	0.001	0.002	0.001	0.000	0.000	0.000	0.001	0.001	0.002	0.002
Mg	0.016	0.018	0.017	0.019	0.009	0.010	0.008	0.006	0.005	0.009	0.010	0.008	0.003	0.005	0.006	0.004	0.005	0.003	0.003
Ca	0.956	0.935	0.959	0.942	0.859	0.820	0.959	0.949	0.763	0.952	0.974	0.978	0.996	0.989	0.957	0.964	0.901	0.893	0.920
Ba	0.000	0.000	0.001	0.001	0.003	0.005	0.000	0.001	0.002	0.000	0.000	0.000	0.001	0.000	0.000	0.001	0.000	0.000	0.000
Na	0.018	0.025	0.028	0.044	0.048	0.041	0.023	0.027	0.060	0.019	0.023	0.028	0.007	0.018	0.040	0.024	0.113	0.120	0.073
K	0.022	0.039	0.022	0.032	0.086	0.120	0.017	0.018	0.182	0.013	0.017	0.024	0.007	0.011	0.019	0.012	0.012	0.011	0.014
Total of cations	5.005	5.007	5.013	5.023	5.007	5.000	5.001	5.003	5.014	5.002	5.024	5.025	4.999	5.011	5.010	5.003	5.014	5.016	5.005
End-members																			
$CaAl_2Si_2O_8$	96.0	93.6	95.0	92.4	86.2	83.2	96.0	95.4	75.8	96.8	96.0	95.0	98.5	97.1	94.2	96.3	87.7	87.2	91.4
$NaAlSi_3O_8$	1.8	2.5	2.7	4.3	4.8	4.1	2.3	2.7	5.9	1.9	2.2	2.7	0.7	1.8	4.0	2.4	11.0	11.7	7.2
$KAlSi_3O_8$	2.1	3.8	2.1	3.0	8.4	11.8	1.7	1.8	17.7	1.3	1.6	2.3	0.7	1.1	1.8	1.2	1.2	1.1	1.3
$K(Fe,Mg)_{0.5}Si_{3.5}O_8$	0.1	0.1	0.1	0.1	0.2	0.4	0.0	0.0	0.4	0.0	0.1	0.1	0.0	0.0	0.0	0.0	0.0	0.0	0.0
$BaAl_2Si_2O_8$	0.0	0.0	0.1	0.1	0.3	0.5	0.0	0.1	0.2	0.0	0.0	0.0	0.1	0.0	0.0	0.1	0.0	0.0	0.0

Note. Electron microprobe analysis; all iron as FeO; Sr is below detection limit.
***Plagioclase in contact with acidic glass.**

Fig. 1. *a* **– Crystal Al-spinel inclusions (1–5 μm in size) in the core of plagioclase from massive parabasalt (sample KR-6). Transmitted light;** *b* **– kirschsteinite and fayalite in a young association of veined parabasalt (leucite + fayalite + kirschteinite + apatite + hedenbergite + sulfides), sample 42-17. Reflected light;** *c* **– symplectitic aggregate of fayalite and kirschsteinite localized between the crystals of leucite, apatite, and clinopyroxene in veined parabasalt (sample 42-17). Transmitted light;** *d* **– zonal spinel crystal in veined parabasalt (sample 42-17). Core – Al-spinel, rim – magnetite with exsolution structures. Reflected light. Spl – Al-spinel, Pl – plagioclase, Ol – Mg-Fe-olivine, Ap – apatite, Lct – leucite, Fa – fayalite, Kir – kirschsteinite, Hd – hedenbergite, Po – pyrrhotite, Py – pyrite, Ti-Mag – titanomagnetite.**

concentrations in fayalite (4.5–7.5 wt.%) and minimum ones in Mg-Fe-olivine at the contact with annealed mudstone (0.02–0.12 wt.%). It is worth noting that some grains of Mg-Fe-olivine and fayalite from massive varieties contain high contents of P_2O_5 (0.4–0.7 wt.%). Earlier, P-bearing olivines (to 6 wt.% P_2O_5) were found in stony-iron meteorites (pallasites) [20] and in specific terrestrial environments – at the contact of basic and normal intrusions with country rocks [21, 22]. The incorporation of phosphorus into the olivine structure is, most likely, associated with two isomorphous schemes with the appearance of vacancies in the octahedral and tetrahedral positions: $M^{2+} + 2Si^{4+} \leftrightarrow \square + 2P^{5+}$; $5Si^{4+} \leftrightarrow 4P^{5+} + \square$.

However, by analogy with apatite [23], it is also possible that phosphorus may substitute for silicon without formation of vacancies (at the balance of charges): $4[SiO_4]^{4-} \leftrightarrow 2[P_2O_7]^{4-}$.

Kirschsteinite occurs in parabasalt dropstone and veined parabasalts as single grains in close association with fayalite (see Fig. 1, *b*, *c*). Veined varieties also contain their oriented intergrowths similar to symplectitic ones. Such intergrowths occur in the rims of large (>100 μm) fayalite and kirschsteinite grains. The composition of the mineral differs considerably from theoretical one ($CaFeSiO_4$) in a lower content of Ca (0.68–0.87 a.f.u.), whose deficiency is compensated for by the incorporation of Fe^{2+} (Table 6) [24]. Constant admixtures are MgO (0.3–4.3 wt.%), MnO (0.8–1.6 wt.%), and P_2O_5 (to 0.4 wt.%). In general, single grains

Table 3

Chemical Composition (wt.%) of Clinopyroxes from Parabasalts of the Southern Urals

Component	Parabasalt dropstone					Massive parabasalt					Veined parabasalt								
	Sample 0107					Sample KR-5	Sample KR-6				Sample 42-17								
		core	rim			core			core	rim			core	rim					
SiO_2	42.99	43.25	46.09	42.49	47.06	50.60	49.49	49.34	48.50	48.55	50.67	45.17	45.29	40.50	48.70	47.89	46.03	45.30	45.81
TiO_2	1.54	1.18	0.74	1.10	0.39	0.63	0.71	0.93	0.85	1.08	0.58	1.43	1.20	2.17	1.10	1.02	0.41	0.10	0.02
Cr_2O_3	0.03	0.00	0.00	0.01	0.01	0.26	0.03	0.00	0.10	0.08	0.13	0.04	0.03	0.00	0.06	0.03	0.00		
Al_2O_3	11.78	11.28	7.79	12.35	7.00	4.68	4.49	3.20	4.30	4.25	1.82	12.85	10.77	13.85	3.50	5.27	4.07	5.81	3.74
FeO	11.94	12.65	13.72	13.84	16.85	7.60	9.11	11.63	11.63	13.04	13.22	4.84	7.61	11.43	14.35	12.98	22.08	25.16	26.22
MnO	0.16	0.23	0.31	0.24	0.46	0.23	0.25	0.32	0.27	0.31	0.33	0.09	0.12	0.16	0.29	0.21	0.57	0.61	0.97
MgO	8.78	9.26	8.99	8.11	7.29	13.63	13.57	12.58	12.23	10.70	13.43	11.10	10.53	7.12	10.50	9.44	3.94	1.13	0.35
CaO	22.00	21.25	21.41	21.41	20.93	22.52	22.17	22.04	22.50	22.29	19.41	24.44	24.36	23.51	21.42	23.14	22.42	21.54	22.26
Na_2O	0.05	0.05	0.04	0.05	0.04	0.07	0.04	0.05	0.03	0.03	0.04	0.03	0.01	0.02	0.01	0.05	0.07	0.14	0.34
Total	99.26	99.15	99.09	99.60	100.03	100.22	99.85	100.09	100.42	100.33	99.63	99.99	99.91	98.77	99.93	100.02	99.59	99.80	99.72
Fe_2O_3	3.72	4.50	2.13	4.88	0.78	0.26	2.58	3.35	4.36	2.31	1.60	0.96	2.78	4.58	1.81	1.88	3.71	1.98	3.48
FeO	8.59	8.60	11.81	9.45	16.15	7.36	6.79	8.61	7.70	10.96	11.78	3.97	5.11	7.31	12.73	11.29	18.74	23.38	23.09
Total	99.63	99.60	99.31	100.09	100.11	100.24	100.11	100.43	100.86	100.56	99.79	100.08	100.19	99.22	100.11	100.21	99.96	99.99	100.07
Formula calculated for 4 cations and 6 oxygens																			
Si	1.639	1.650	1.773	1.622	1.819	1.875	1.846	1.857	1.819	1.841	1.920	1.668	1.690	1.558	1.863	1.827	1.839	1.834	1.869
Al^{IV}	0.361	0.350	0.227	0.378	0.181	0.125	0.154	0.142	0.181	0.159	0.080	0.332	0.310	0.442	0.137	0.173	0.161	0.166	0.131
Al^{VI}	0.168	0.157	0.126	0.178	0.138	0.080	0.044	0.000	0.009	0.031	0.001	0.227	0.164	0.186	0.021	0.063	0.031	0.111	0.049
Ti	0.044	0.034	0.021	0.032	0.011	0.018	0.020	0.026	0.024	0.031	0.016	0.040	0.034	0.063	0.032	0.029	0.012	0.003	0.001
Cr	0.001	0.000	0.000	0.000	0.000	0.008	0.001	0.000	0.003	0.002	0.004	0.001	0.001	0.000	0.002	0.001	0.000		
Fe^{3+}	0.107	0.129	0.062	0.140	0.023	0.007	0.072	0.095	0.123	0.066	0.046	0.027	0.078	0.133	0.052	0.054	0.112	0.060	0.107
Fe^{2+}	0.274	0.274	0.380	0.302	0.522	0.228	0.212	0.271	0.242	0.348	0.373	0.123	0.159	0.235	0.407	0.360	0.626	0.791	0.788
Mn	0.005	0.008	0.010	0.008	0.015	0.007	0.008	0.010	0.009	0.010	0.010	0.003	0.004	0.005	0.009	0.007	0.019	0.021	0.033
Mg	0.499	0.526	0.515	0.461	0.420	0.753	0.754	0.706	0.684	0.605	0.758	0.611	0.586	0.408	0.599	0.537	0.235	0.068	0.021
Ca	0.899	0.869	0.882	0.876	0.867	0.894	0.886	0.889	0.904	0.906	0.788	0.967	0.974	0.969	0.878	0.946	0.960	0.934	0.973
Na	0.003	0.003	0.003	0.004	0.003	0.005	0.003	0.004	0.002	0.002	0.003	0.002	0.001	0.002	0.001	0.003	0.006	0.011	0.027
Ca + Na	0.902	0.872	0.886	0.879	0.870	0.900	0.889	0.893	0.907	0.908	0.791	0.969	0.975	0.970	0.879	0.949	0.965	0.945	1.000
Mg#	0.57	0.57	0.54	0.51	0.44	0.76	0.73	0.66	0.65	0.59	0.64	0.80	0.71	0.53	0.57	0.56	0.24	0.07	0.02
Mg*	0.65	0.66	0.58	0.60	0.45	0.77	0.78	0.72	0.74	0.64	0.67	0.83	0.79	0.63	0.60	0.60	0.27	0.08	0.03

Note. Mg# — $Mg/(Mg + Fe_{tot})$ in a.f.u.; Mg* — $Mg/(Mg + Fe^{2+})$ in a.f.u.

Table 4

Chemical Composition (wt.%) of Low-Calcium Pyroxenes from Veined Parabasalt (Sample 42–17)

Component	Orthopyroxene (?)								Pigeonite								Subcalcic augite		
SiO_2	50.33	50.02	50.52	52.23	50.91	51.00	50.96	48.45	50.04	50.29	49.96	50.39	50.98	50.79	49.95	48.45	49.91	50.92
TiO_2	0.48	0.40	0.35	0.30	0.37	0.30	0.31	0.79	0.37	0.44	0.56	0.44	0.35	0.47	0.52	0.77	0.51	0.44
Cr_2O_3	0.61	0.14	0.18	0.17	0.12	0.29	0.15		0.08	0.13		0.06	0.11	0.08	0.08	0.02	0.09	0.14
Al_2O_3	2.09	2.23	1.51	1.52	1.57	1.38	1.51	2.28	0.56	0.73	1.00	1.08	1.23	0.98	1.21	1.35	1.58	1.61
FeO	26.00	28.14	26.50	20.12	25.39	24.26	24.07	33.95	30.39	29.54	29.21	27.54	25.45	26.09	27.35	29.20	22.09	16.09
MnO	0.85	0.60	0.59	0.61	0.57	0.57	0.52	0.60	0.61	0.60	0.57	0.58	0.54	0.62	0.60	0.68	0.54	0.42
MgO	18.42	16.95	18.31	22.45	18.87	19.30	19.44	13.21	12.36	13.01	13.07	14.44	15.98	14.97	13.77	8.37	13.18	14.57
CaO	1.28	1.38	1.70	1.90	2.09	2.20	2.24	0.66	5.53	5.54	5.36	5.57	5.74	6.30	6.48	10.87	11.77	15.55
Na_2O	0.06	0.03	0.02	0.05	0.01	0.01	0.02	0.04	0.02	0.02	0.07	0.00	0.08	0.02	0.04	0.07	0.05	0.03
Total	100.12	99.88	99.68	99.35	99.90	99.31	99.22	99.97	99.96	100.30	99.80	100.10	100.46	100.33	100.00	99.79	99.72	99.76
Fe_2O_3	1.12	0.77	1.42	0.76	1.25	0.96	1.12	0.51	0.03	0.02	0.05	0.38	1.05	0.47	0.87	0.49	1.46	1.38
FeO	24.99	27.45	25.22	19.44	24.26	23.40	23.06	33.49	30.36	29.52	29.16	27.20	24.50	25.66	26.57	28.76	20.78	14.85
Total	100.23	99.95	99.82	99.42	100.03	99.41	99.33	100.02	99.97	100.30	99.80	100.14	100.57	100.37	100.09	99.84	99.87	99.90
Formula calculated for 4 cations and 6 oxygens																		
Si	1.917	1.926	1.934	1.947	1.935	1.943	1.940	1.917	1.975	1.969	1.962	1.956	1.949	1.957	1.945	1.940	1.929	1.931
Al^{IV}	0.083	0.074	0.066	0.053	0.065	0.057	0.060	0.083	0.025	0.031	0.038	0.044	0.051	0.043	0.055	0.060	0.071	0.069
Al^{VI}	0.011	0.027	0.002	0.014	0.005	0.005	0.008	0.023	0.001	0.003	0.009	0.005	0.004	0.002	0.000	0.004	0.001	0.003
Ti	0.014	0.011	0.010	0.008	0.010	0.009	0.009	0.023	0.011	0.013	0.017	0.013	0.010	0.014	0.015	0.023	0.015	0.013
Cr	0.018	0.004	0.006	0.005	0.004	0.009	0.004		0.003	0.004		0.002	0.003	0.002	0.002	0.001	0.003	0.004
Fe^{3+}	0.032	0.022	0.041	0.021	0.036	0.027	0.032	0.015	0.001	0.001	0.002	0.011	0.030	0.014	0.026	0.015	0.042	0.039
Fe^{2+}	0.796	0.884	0.807	0.606	0.771	0.746	0.734	1.108	1.002	0.967	0.958	0.883	0.783	0.827	0.865	0.963	0.671	0.471
Mn	0.027	0.020	0.019	0.019	0.018	0.018	0.017	0.020	0.020	0.020	0.019	0.019	0.018	0.020	0.020	0.023	0.018	0.013
Mg	1.045	0.973	1.044	1.247	1.069	1.096	1.103	0.779	0.727	0.759	0.765	0.835	0.910	0.860	0.799	0.499	0.759	0.823
Ca	0.052	0.057	0.070	0.076	0.085	0.090	0.091	0.028	0.234	0.232	0.226	0.232	0.235	0.260	0.270	0.466	0.487	0.632
Na	0.005	0.002	0.001	0.004	0.001	0.001	0.002	0.003	0.001	0.002	0.006	0.000	0.006	0.002	0.003	0.006	0.004	0.002
Ca#	0.03	0.03	0.04	0.04	0.04	0.05	0.05	0.01	0.12	0.12	0.11	0.12	0.12	0.13	0.14	0.24	0.25	0.32
Mg#	0.56	0.52	0.55	0.67	0.57	0.59	0.59	0.41	0.42	0.44	0.44	0.48	0.53	0.51	0.47	0.34	0.52	0.62

Note. Ca# — $Ca/(Ca + Mg + Fe_{tot} + Mn)$ in a.f.u.; Mg# — $Mg/(Mg + Fe_{tot})$ in a.f.u.

Table 5

Chemical Composition (wt.%) of Olivines from Parabasalts of the Southern Urals

Component	Parabasalt dropstone				Massive parabasalt										Veined parabasalt						
	Sample 0107				Sample KR-5					Sample KR-6					Sample 42-17					Sample 063-45	
	core	rim			core	rim	core	rim		core	rim							sym	sym	core	rim
SiO_2	32.22	31.99	31.24	30.95	32.65	31.62	31.90	31.32	30.61	34.24	33.66	35.22	31.08	29.28	35.91	32.92	31.58	30.98	31.07	30.67	30.26
TiO_2	0.00	0.01	0.06	0.06	0.03	0.03	0.04	0.08	0.08	0.00	0.01	0.01	0.05	0.11	0.03	0.02	0.01	0.00	0.04	0.03	0.02
FeO	52.07	53.52	57.72	59.34	49.88	53.05	55.97	58.32	61.63	39.82	44.88	34.95	58.45	66.63	36.26	50.07	57.78	58.79	57.87	60.78	63.22
MnO	1.22	1.17	1.70	2.34	1.25	1.36	1.34	1.48	1.61	0.88	1.10	0.64	1.25	1.80	0.62	0.77	0.99	1.45	1.46	1.89	2.05
MgO	11.19	10.58	5.95	6.44	15.34	12.98	9.26	7.07	5.65	24.26	19.16	28.10	8.08	0.83	25.49	15.71	8.56	2.79	2.96	5.94	3.72
CaO	3.14	2.27	2.76	0.58	0.73	0.72	0.65	0.63	0.85	0.77	0.77	0.55	0.76	1.40	1.41	0.39	0.35	5.80	6.41	0.00	0.00
NiO															0.05						
P_2O_5												0.69	0.28				0.13	0.08	0.07		
Total	99.84	99.54	99.43	99.70	99.88	99.75	99.16	98.90	100.43	99.97	99.58	100.15	99.96	100.05	99.77	99.87	99.40	99.89	99.88	99.31	99.27
Formula calculated for 4 oxygens																					
Si	0.999	1.000	1.007	1.000	0.991	0.981	1.010	1.010	0.991	0.982	0.996	0.977	0.989	0.987	1.010	0.996	1.005	1.008	1.008	1.000	1.003
Ti	0.000	0.000	0.002	0.001	0.001	0.001	0.001	0.002	0.002	0.000	0.000	0.000	0.001	0.003	0.001	0.000	0.000	0.000	0.001	0.001	0.000
Fe	1.350	1.399	1.556	1.603	1.266	1.377	1.483	1.573	1.668	0.955	1.111	0.811	1.556	1.878	0.853	1.267	1.537	1.600	1.570	1.657	1.752
Mn	0.032	0.031	0.046	0.064	0.032	0.036	0.036	0.040	0.044	0.021	0.028	0.015	0.034	0.051	0.015	0.020	0.027	0.040	0.040	0.052	0.058
Mg	0.517	0.493	0.286	0.310	0.694	0.600	0.437	0.340	0.273	1.037	0.845	1.162	0.383	0.042	1.069	0.708	0.406	0.135	0.143	0.289	0.184
Ca	0.104	0.076	0.095	0.020	0.024	0.024	0.022	0.022	0.029	0.024	0.025	0.016	0.027	0.051	0.042	0.013	0.012	0.202	0.223	0.000	0.000
P												0.016	0.008				0.004	0.002	0.002		
Total of cations	3.001	3.000	2.992	2.999	3.008	3.018	2.989	2.988	3.007	3.018	3.004	2.998	2.999	3.011	2.989	3.004	2.990	2.988	2.988	2.999	2.997
100Fe/(Fe + Mn + Mg)	71.09	72.76	82.40	81.08	63.56	68.40	75.81	80.53	84.05	47.44	56.00	40.79	78.86	95.28	44.05	63.51	78.04	90.13	89.55	82.94	87.90
End-members																					
Mg_2SiO_4	25.81	24.66	14.41	15.52	34.42	29.47	22.10	17.21	13.53	50.90	42.08	57.97	19.17	2.06	54.03	35.29	20.48	6.84	7.24	14.44	9.22
Fe_2SiO_4	67.39	69.99	78.44	80.27	62.80	67.60	74.97	79.64	82.82	46.89	55.32	40.46	77.80	92.90	43.08	63.11	77.57	80.91	79.45	82.94	87.90
Mn_2SiO_4	1.60	1.55	2.34	3.21	1.59	1.76	1.82	2.05	2.19	1.05	1.37	0.75	1.69	2.54	0.75	0.98	1.35	2.02	2.03	2.61	2.89
Ca_2SiO_4	5.21	3.80	4.81	1.00	1.18	1.17	1.11	1.10	1.46	1.16	1.22	0.81	1.35	2.50	2.15	0.63	0.60	10.23	11.28	0.00	0.00

Note. Electron microprobe analysis; all iron as FeO; Cr, Al, Na, K are below detection limits; sym — symplectite intergrowths with kirschsteinite.

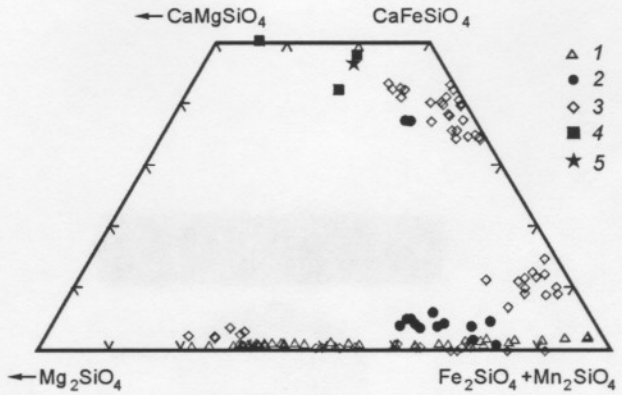

Fig. 2. Composition diagram of olivines and kirschsteinites from technogenic parabasalts. *1* – massive parabasalts; *2* – parabasalt dropstone; *3* – veined parabasalts; *4* – natural magnesian kirschsteinites [29–31], *5* – kirschsteinite from meteorites [26].

from dropstone and veined parabasalt are richer in MgO than the mineral from symplectites (3.7–4.3 and 0.3–2.0 wt.%, respectively). The largest grains from veinlets have a chemical zoning viewed as a decrease in contents of CaO, MgO, and P_2O_3 and an increase in concentrations of FeO and MnO from core to rim (see Table 6). The incorporation of phosphorus into the structure seems to be related to isomorphous substitutions typical of olivine [21, 22]. According to literature data [24–27], there are two groups of kirschsteinites by contents of CaO and FeO: 1) with excess of the fayalite end-member; 2) with excess of the larnite end-member. As far as we know, fayalitic kirschsteinite (f = 82–96) from parabasalts of the Southern Urals is the only finding of this mineral in the terrestrial environments. A compositionally similar phase was earlier found in angrites and other stony meteorites [26, 27]. At the same time, $CaFeSiO_4$ is a common component of fluxed metallurgic slags [24], and glasses of close compositions exist in ashes of TPS [28]. Natural magnesian kirschsteinite containing 50 to 77 mol.% $CaFeSiO_4$ was found in melilite nephelinites from Shaheru (Zaire) and in garnet-wollastonite-melilite skarns of the Tazheran alkaline massif (Baikal region) [29–31]. Monticellites with 10–40 mol.% $CaFeSiO_4$ are characteristic of alkaline-basic rocks (alnoites, kamafugites, and carbonatites).

Al-spinel and titanomagnetite are the main ore minerals. Al-spinel is the earliest phase and occurs as crystallites in anorthite, Mg-clinopyroxene, and Mg-olivine (see Fig. 1, *a*). Titanomagnetite crystallizes after them and occurs together with pyrrhotite in later fayalite, kirschsteinite, and Fe-clinopyroxene. Typical zonal grains contain Al-spinel in the core and titanomagnetite in the rim (see Fig. 1, *d*). Al-spinel corresponds to Fe-rich ($Mg/(Mg + Fe^{2+})$ = 0.28–0.47) members of the $MgAl_2O_4$–$FeAl_2O_4$ series with minor contents of magnetite (Fe_2O_3 – 5–21 wt.%) and ulvospinel (TiO_2 < 1.3 wt.%) end-members (Table 7, Fig. 3). In veined parabasalts, magnetites of the first generation have high concentrations of Al_2O_3 (7–13 wt.%), moderate ones of TiO_2 (4.5–7.7 wt.%), and low contents of MgO (0.1–0.5 wt.%). The $Fe^{2+}/(Fe^{2+} + Fe^{3+})$ value varies from 0.38 to 0.53. Later magnetites from interstices contain more TiO_2 (10–22 wt.%). In massive parabasalts, large (>100 μm) grains have concentrations of TiO_2 from 13.5 to 14.5 wt.%, while later small grains have a maximum content of TiO_2 (24–29 wt.%) and approach in composition ulvospinel. Crystals from massive and veined parabasalts contain exsolutional structures of ilmenite (or ulvospinel), whereas individuals from dropstone lack them.

Apatite in parabasalts is a late mineral and is associated with potassium phases (acidic glass, K-feldspar, and leucite), fayalite, kirschsteinite, and titanomagnetite (see Fig. 1, *c*). In veined parabasalts it forms crystals in interstices and crystallites in fayalite, kirschsteinite, hedenbergite, and titanomagnetite. Compositions of apatites from different types of parabasalts differ considerably. Fluorapatite is typical of dropstone and oxyfluorapatite – of massive parabasalts. It is difficult to refer apatites from veinlets to a particular variety (Table 8). The contents of F (0.06–1.63 wt.%) and Cl (to 0.7 wt.%) and deficiency of totals in a number of analyses (97.17–97.94 wt.%) suggest the presence of an underdetermined element here. Because of small crystal sizes (to 5–10 μm), we failed to perform IR-spectroscopic studies and thus to prove or disprove the presence of (OH)-groups in apatite. Noteworthy is, however, that no hydroxyl-containing minerals have been found in initial associations of fused rocks by now [7, 18, 23]. According to data from [23], dry high-temperature

Table 6

Chemical Composition (wt.%) of Kirschsteinites from Parabasalts of the Southern Urals

Component	Parabasalt dropstone	Veined parabasalt													
	Sample 0107	Sample 42-17													
			c	m	r		*	sym	sym	sym	sym	sym	sym	sym	sym	sym
SiO_2	32.16	32.71	32.24	32.35	32.26	31.54	32.82	31.96	31.81	31.85	31.82	32.02	31.68	32.01	31.78	31.74
TiO_2	0.02	0.04	0.02	0.01	0.02	0.04	0.06	0.00	0.05	0.00	0.01	0.00	0.03	0.00	0.01	0.05
FeO	39.86	39.59	35.93	36.68	37.87	40.09	37.04	41.41	41.54	42.80	44.41	41.34	46.03	42.02	43.80	43.73
MnO	1.08	1.11	0.85	0.91	0.98	1.35	0.81	0.98	1.10	1.29	1.34	1.44	1.51	1.48	1.60	1.28
MgO	4.30	4.30	3.99	3.95	3.71	2.06	3.38	1.39	2.66	0.38	1.78	0.32	0.39	1.40	1.45	1.75
CaO	22.76	22.58	26.39	25.82	24.91	23.88	25.58	23.38	22.04	23.33	20.18	23.84	19.94	22.50	20.96	21.03
Na_2O			0.05	0.05	0.02											
P_2O_5			0.39	0.20	0.14	0.22	0.24	0.14	0.26	0.10	0.25	0.07	0.15	0.14	0.18	0.23
Total	100.18	100.33	99.85	99.97	99.91	99.18	99.93	99.26	99.45	99.74	99.79	99.04	99.72	99.55	99.78	99.81
Formula calculated for 4 oxygens																
Si	0.994	1.005	0.989	0.994	0.996	0.994	1.007	1.008	0.998	1.008	1.004	1.016	1.010	1.009	1.004	1.001
Ti	0.000	0.001	0.000	0.000	0.000	0.001	0.001	0.000	0.001	0.000	0.000	0.000	0.001	0.000	0.000	0.001
Fe	1.031	1.018	0.922	0.943	0.978	1.057	0.951	1.092	1.090	1.133	1.172	1.097	1.228	1.108	1.158	1.153
Mn	0.028	0.029	0.022	0.024	0.026	0.036	0.021	0.026	0.029	0.035	0.036	0.039	0.041	0.040	0.043	0.034
Mg	0.198	0.197	0.182	0.181	0.171	0.097	0.155	0.065	0.124	0.018	0.084	0.015	0.018	0.066	0.068	0.082
Ca	0.754	0.744	0.868	0.850	0.824	0.806	0.841	0.790	0.741	0.791	0.682	0.811	0.681	0.760	0.710	0.711
Na			0.003	0.003	0.001											
P			0.010	0.005	0.004	0.006	0.006	0.004	0.007	0.003	0.007	0.002	0.004	0.004	0.005	0.006
Total of cations	3.005	2.994	2.997	3.000	2.999	2.991	2.976	2.982	2.983	2.985	2.979	2.979	2.979	2.982	2.983	2.983
100Fe/(Fe+Mn+Mg)	81.99	81.84	81.85	82.18	83.28	88.84	84.40	92.27	87.66	95.59	90.75	95.33	95.41	91.32	91.24	90.83
Formula calculated for end-members of the olivine group																
Mg_2SiO_4	9.85	9.91	9.14	9.04	8.54	4.85	7.86	3.31	6.27	0.89	4.24	0.77	0.93	3.33	3.45	4.15
Fe_2SiO_4	51.25	51.21	46.17	47.12	48.91	52.94	48.32	55.34	54.93	57.32	59.38	55.93	62.38	56.15	58.51	58.24
Mn_2SiO_4	1.41	1.45	1.11	1.18	1.28	1.81	1.08	1.32	1.47	1.75	1.81	1.97	2.07	2.00	2.16	1.73
Ca_2SiO_4	37.49	37.42	43.45	42.50	41.22	40.40	42.75	40.03	37.33	40.03	34.57	41.33	34.62	38.52	35.87	35.88
Formula calculated for end-members of the monticellite group																
$CaMgSiO_4$	19.81	19.70	18.25	18.09	17.07	9.67	15.46	6.53	12.44	1.77	8.37	1.51	1.83	6.58	6.83	8.23
$CaMnSiO_4$	2.83	2.89	2.21	2.36	2.55	3.60	2.12	2.61	2.91	3.46	3.58	3.87	4.08	3.95	4.28	3.42
$CaFeSiO_4$	52.75	51.78	66.31	64.56	62.77	67.36	66.54	69.88	58.73	73.91	56.29	75.71	62.23	65.46	59.87	59.42
Fe_2SiO_4	25.15	25.00	12.94	14.85	17.50	19.15	14.26	19.68	25.13	19.70	30.47	17.02	30.27	22.65	27.95	27.96
Exsessive SiO_2		0.64	0.132	0.046	0.054	0.14	1.55	1.24	0.70	1.13	1.20	1.87	1.55	1.31	1.00	0.90
Total of end-members	100.54	100.00	99.84	99.89	99.94	99.93	99.92	99.95	99.91	99.97	99.92	99.98	99.95	99.95	99.94	99.92

Note. Electron microprobe analysis; all iron as FeO; Ni, Cr, Al, and K are below detection limits; c, m, r — core, middle, and rim of grain; sym — symplectite intergrowths with fayalite.

***Phase from polycrystalline inclusion in plagioclase.**

Table 7

Chemical Composition (wt.%) of Al-Spinel, Magnetite, and Ilmenite from Parabasalts of the Southern Urals

Component	Parabasalt dropstone	Massive parabasalt					Veined parabasalt																	
	Sample 0107	Sample KR-5			Sample KR-6					Sample 42-17														
	Sp	Mgn	Mgn	Sp*	Sp	Mgn	Mgn	Mgn	Mgn	Mgn	Sp*	Sp*	Sp	Sp	Mgn	Mgn	Mgn	Mgn$^{\$}$	Mgn	Mgn	Mgn	Mgn	Ilm$^{\#}$	Ilm	Ilm$^{\$}$
SiO_2				0.12	0.10	0.13	0.15	0.17	0.13	0.14							0.09		0.14	0.18	0.11	0.17	0.03		
TiO_2	0.58	1.46	0.68	0.38	0.76	22.94	23.43	13.57	28.36	29.13	0.37	0.48	0.26	0.46	1.96	4.57	5.73	6.77	10.17	14.29	19.02	22.05	47.34	47.35	46.95
Cr_2O_3	0.33	0.08	0.03	0.43	0.13	0.02	0.00		0.00	0.00	0.57	0.51	0.15	0.00	0.00	0.00	0.07	0.00	0.04	0.02	0.06	0.00		0.14	0.09
V_2O_3	0.15	0.03	0.02	0.32	0.46						0.13	0.44	0.04	0.00	0.00	0.01		0.00						0.33	0.36
Al_2O_3	42.77	19.28	7.99	58.33	55.87	1.83	1.86	4.34	1.75	1.61	56.15	53.49	57.62	53.29	4.77	9.33	4.80	9.17	3.49	2.12	0.70	1.50	0.18	0.22	0.31
FeO	45.03	70.26	82.79	28.25	30.00	71.34	71.09	76.30	67.05	66.30	29.92	33.45	30.01	37.67	86.50	79.65	80.53	78.54	79.03	78.29	74.49	72.35	49.91	49.08	49.45
MnO	0.60	0.48	0.41	0.31	0.28	0.68	0.64	0.40	0.76	0.78	0.37	0.25	0.31	0.34	0.44	0.44	0.65	0.54	0.02	0.33	0.24	0.71	0.34	0.53	0.46
MgO	7.73	3.79	2.16	11.38	11.26	0.35	0.36	1.39	0.12	0.12	11.50	9.99	10.66	7.23	0.05	0.45	2.39	0.32	1.73	0.26	1.50	0.23	1.55	1.74	1.71
CaO				0.11	0.13	0.33	0.28	0.01	0.15	0.35							0.09		0.12	0.00	0.08	0.02	0.05		
NiO	0.18	0.00	0.02	0.01	0.09						0.05	0.08	0.05	0.03	0.00	0.00		0.00						0.00	0.02
ZnO	0.12	0.02	0.00	0.07	0.14						0.11	0.08	0.19	0.17	0.10	0.08		0.03						0.00	0.00
Total	97.50	95.40	94.10	99.71	99.21	97.63	97.82	96.18	98.33	98.44	99.15	98.77	99.28	99.18	93.82	94.53	94.35	95.37	94.74	95.49	96.20	97.03	99.41	99.38	99.34
Fe_2O_3	20.95	45.38	59.42	5.23	7.39	23.34	22.22	38.05	12.06	11.29	7.69	9.37	6.20	9.40	59.45	49.02	53.33	45.23	45.67	38.12	31.73	24.05	5.79	5.64	5.98
FeO	26.18	29.42	29.32	23.55	23.35	50.34	51.09	42.06	56.20	56.14	23.00	25.02	24.43	29.21	33.01	35.54	32.55	37.84	37.93	43.99	45.94	50.71	44.70	44.01	44.07
Total	99.60	99.94	100.05	100.23	99.95	99.96	100.04	99.99	99.53	99.57	99.92	99.71	99.90	100.12	99.78	99.44	99.69	99.91	99.32	99.31	99.38	99.44	99.99	99.95	99.94
Formula calculated for 3 cations and 4 oxygens																									
Si				0.003	0.003	0.005	0.006	0.006	0.005	0.005							0.003		0.005	0.007	0.004	0.006	0.001		
Ti	0.013	0.037	0.018	0.008	0.016	0.642	0.654	0.375	0.794	0.815	0.008	0.010	0.005	0.010	0.055	0.125	0.158	0.185	0.284	0.405	0.536	0.622	0.888	0.887	0.879
Cr	0.008	0.002	0.001	0.009	0.003	0.001	0.000	0.000	0.000	0.000	0.012	0.011	0.003	0.000	0.000	0.000	0.002	0.000	0.001	0.001	0.002	0.000		0.003	0.002
V	0.004	0.001	0.001	0.007	0.010			0.000			0.003	0.010	0.001	0.000	0.000	0.000		0.000						0.006	0.007
Al	1.495	0.768	0.341	1.862	1.806	0.080	0.081	0.188	0.077	0.071	1.811	1.762	1.858	1.780	0.211	0.402	0.208	0.393	0.153	0.094	0.031	0.066	0.005	0.006	0.009
Fe^{3+}	0.468	1.155	1.620	0.106	0.152	0.653	0.621	1.051	0.338	0.316	0.158	0.197	0.128	0.200	1.678	1.347	1.474	1.237	1.277	1.081	0.894	0.679	0.109	0.106	0.112
Fe^{2+}	0.649	0.832	0.889	0.533	0.536	1.566	1.587	1.291	1.750	1.747	0.527	0.585	0.559	0.692	1.036	1.085	1.000	1.150	1.179	1.387	1.439	1.590	0.932	0.916	0.918
Mn	0.015	0.014	0.013	0.007	0.007	0.022	0.020	0.012	0.024	0.025	0.008	0.006	0.007	0.008	0.014	0.013	0.020	0.017	0.001	0.011	0.008	0.023	0.007	0.011	0.010
Mg	0.342	0.191	0.117	0.459	0.460	0.019	0.020	0.076	0.007	0.007	0.469	0.416	0.435	0.305	0.003	0.025	0.131	0.017	0.096	0.015	0.084	0.013	0.058	0.065	0.063
Ca				0.003	0.004	0.013	0.011	0.000	0.006	0.014							0.004		0.005	0.000	0.003	0.001	0.002		
Ni	0.004	0.000	0.001	0.000	0.002			0.000			0.001	0.002	0.001	0.001	0.000	0.000	0.000	0.000	0.000	0.000	0.000	0.000		0.000	0.000
Zn	0.003	0.000	0.000	0.001	0.003			0.000			0.002	0.002	0.004	0.004	0.003	0.002	0.000	0.001	0.000	0.000	0.000	0.000		0.000	0.000
R^{2+}	1.013	1.037	1.018	1.005	1.011	1.606	1.626	1.380	1.781	1.779	1.008	1.010	1.005	1.010	1.055	1.125	1.151	1.185	1.275	1.412	1.530	1.626	0.999	0.992	0.991
R^{3+}	1.987	1.963	1.982	1.995	1.989	1.380	1.362	1.620	1.213	1.207	1.992	1.990	1.995	1.990	1.945	1.875	1.845	1.815	1.720	1.588	1.467	1.373	1.001	1.008	1.009

Note. Electron microprobe analysis; all iron as FeO. Minerals: Sp — Al-spinel, Mgn — magnetite, Ilm — ilmenite. Ilmenite formula is calculated for 2 cations and 3 cations. R^{2+} is total of bivalent cations; R^{3+} is total of trivalent cations, Si, and Ti.

*** Crystallites of Al-spinel in plagioclase; $ is the magnetite + ilmenite association; # is a single lath in glass.**

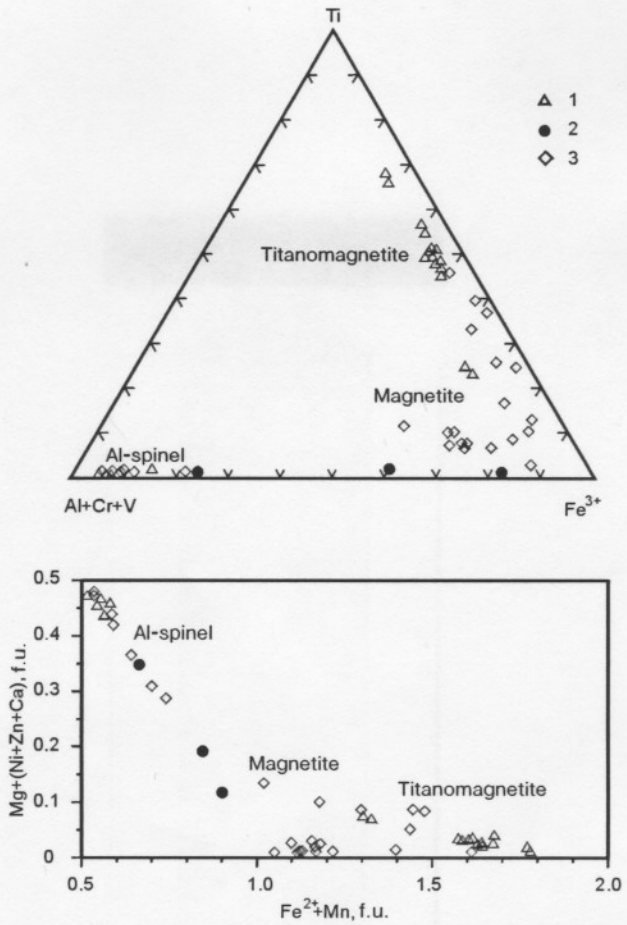

Fig. 3. Composition diagram of spinels from technogenic parabasalts. *1* — massive parabasalts, *2* — parabasalt dropstone, *3* — veined parabasalts.

conditions favor the incorporation of carbonate ion into the apatite structure, $2(OH,F,Cl)^- \rightarrow (CO3)^{2-} + \square$, fairly probable in our samples as well.

All the individuals have elevated contents of FeO (0.5–3.7 wt.%) and SiO_2 (to 6.4 wt.%) at extremely low concentrations of rare earths (below detection limit) and Y_2O_3 (<0.3 wt.%), which, most likely, reflects initially minor amounts of these elements in carboniferous sediments. Interesting is the incorporation of Si into to the apatite structure, because in this case traditional isomorphous substitutions for Si appeared to be unsuitable [33]. Recent data [23] show that the structure of high-temperature apatites is characterized by the presence of pyrophosphate group $[P_2O_7]^{4-}$. We think that the following schemes of isomorphism are the most probable:

$3[PO_4]^{3-} + F^- \Leftrightarrow [P_2O_7]^{4-} + [SiO_4]^{4-} + O^{2-}$ – veined parabasalt,

$4[PO_4]^{3-} \Leftrightarrow [P_2O_7]^{4-} + 2[SiO_4]^{4-}$, $2[PO_4]^{3-} \Leftrightarrow [SiO_4]^{4-} + [CO_3]^{2-}$ – parabasalt dropstone.

Leucite in massive and veined parabasalts forms rather large (to 1 mm) tetragon-trioctahedral crystals in cavities or interstices, and in dropstone mesostasis it occurs as xenomorphic grains (to 20 μm in size). Leucite inclusions have been found in plagioclase of veined parabasalt, which suggests that this mineral crystallized together or somewhat later than plagioclase. Polysynthetic twinning is characteristic of leucite. Its chemical composition is close to the theoretical one (Table 9) but differs in constant presence of Na_2O (to 0.3 wt.%), negligible excess of Si (2.01–2.02 a.f.u.), and deficiency of Al (0.96–0.98 a.f.u.), which is, most likely, compensated for by the incorporation of Fe^{3+} (to 0.06 a.f.u.). Leucite from parabasalt dropstone has high concentrations of Fe_2O_3 (0.6–2.0 wt.%) and BaO (0.4–0.5 wt.%).

In addition to leucite, **nepheline** was found in veined parabasalt. It was accidentally found in association with magnetite, Fe-clinopyroxene, and apatite in a polycrystalline inclusion from the central zone of augite. Its

Table 8

Chemical Composition (wt.%) of Apatites from Parabasalts of the Southern Urals

Component	Parabasalt dropstone				Massive parabasalt					Veined parabasalt								
	Sample 0107				Sample KR-6					Sample 42-17								
	1	1	2	1	3	7	2	1c	1r	1	3	6*	3	2*	3c	1m	1r	1#
SiO_2	4.79	4.58	4.96	3.21	2.34	0.87	0.54	0.82	1.16	5.52	5.51	4.94	6.09	6.35	2.52	4.69	5.92	3.36
P_2O_5	36.62	36.96	36.53	38.47	38.81	40.66	40.99	40.60	40.39	37.29	37.40	37.37	35.07	35.19	40.16	37.81	35.84	38.23
SO_3	0.00	0.00	0.00	0.00	0.00	0.00	0.00	0.00	0.00	0.08	0.00	0.00	0.01	0.04	0.00	0.03	0.02	0.00
Y_2O_3			0.13		0.24	0.17						0.09						
FeO	3.15	3.67	2.44	1.20	0.97	0.66	0.62	0.57	0.90	1.55	1.54	1.71	1.58	2.15	1.20	1.58	2.04	3.08
MnO	0.08	0.04	0.06	0.04	0.07	0.04	0.03	0.04	0.05	0.06	0.04	0.05	0.11	0.12	0.07	0.10	0.12	0.05
MgO	0.28	0.29	0.24	0.22	0.29	0.23	0.20	0.18	0.16	0.21	0.24	0.26	0.14	0.15	0.10	0.17	0.18	0.14
CaO	52.48	51.98	52.56	54.14	54.82	55.42	55.99	55.47	55.24	54.26	53.92	54.18	53.37	53.32	54.83	53.66	52.84	53.15
SrO	0.15	0.15	0.24	0.21	0.11	0.13	0.15	0.12	0.16	0.29	0.20	0.16	0.47	0.36	0.28	0.23	0.38	0.67
Na_2O	0.12	0.08	0.06	0.09	0.02	0.00	0.00	0.07	0.00	0.17	0.11	0.10	0.14	0.15	0.18	0.11	0.15	0.21
F	3.74	3.48	3.29	3.76	2.89	3.27	2.67	3.22	3.50	0.71	1.63	1.58	0.22	0.06	1.21	0.51	0.33	1.00
Cl	0.00	0.00	0.01	0.02	0.01	0.01	0.00	0.00	0.00	0.42	0.24	0.25	0.07	0.13	0.32	0.67	0.27	0.68
Total	101.41	101.23	100.51	101.36	100.56	101.47	101.19	101.09	101.56	100.56	100.82	100.68	97.28	98.00	100.86	99.56	98.08	100.57
$O\text{-}(F,Cl)_2$	1.57	1.47	1.39	1.59	1.22	1.38	1.12	1.36	1.47	0.39	0.74	0.72	0.11	0.05	0.58	0.37	0.20	0.57
Total	99.84	99.76	99.12	99.77	99.34	100.09	100.07	99.73	100.09	100.17	100.08	99.96	97.17	97.94	100.28	99.19	97.88	99.99
Formula calculated for 10 cations in the A position																		
Si	0.802	0.770	0.839	0.537	0.388	0.144	0.088	0.136	0.192	0.915	0.921	0.819	1.026	1.062	0.417	0.788	0.999	0.554
P	5.191	5.257	5.229	5.453	5.447	5.687	5.690	5.685	5.665	5.231	5.292	5.248	4.999	4.984	5.618	5.375	5.121	5.339
S	0.000	0.000	0.000	0.000	0.000	0.000	0.000	0.000	0.000	0.010	0.000	0.000	0.002	0.005	0.000	0.003	0.002	0.000
Y			0.012		0.021	0.015						0.008						
Fe	0.441	0.516	0.344	0.168	0.135	0.091	0.086	0.079	0.125	0.215	0.215	0.238	0.222	0.300	0.166	0.222	0.288	0.425
Mn	0.011	0.006	0.009	0.006	0.009	0.006	0.005	0.006	0.007	0.009	0.005	0.006	0.016	0.017	0.009	0.014	0.017	0.007
Mg	0.070	0.072	0.061	0.055	0.072	0.057	0.049	0.044	0.039	0.052	0.061	0.063	0.035	0.037	0.024	0.043	0.046	0.035
Ca	9.424	9.365	9.532	9.722	9.746	9.818	9.846	9.838	9.814	9.642	9.664	9.637	9.635	9.564	9.716	9.663	9.563	9.402
Sr	0.015	0.015	0.024	0.020	0.011	0.012	0.014	0.012	0.015	0.028	0.019	0.015	0.046	0.035	0.027	0.022	0.037	0.064
Na	0.039	0.026	0.020	0.029	0.006	0.000	0.000	0.022	0.000	0.055	0.037	0.032	0.046	0.047	0.059	0.036	0.049	0.067
F	1.981	1.849	1.757	1.991	1.517	1.709	1.382	1.684	1.834	0.371	0.859	0.830	0.117	0.030	0.632	0.271	0.176	0.522
Cl	0.001	0.000	0.003	0.005	0.002	0.003	0.000	0.000	0.000	0.119	0.068	0.071	0.020	0.036	0.090	0.190	0.077	0.190

Note. Electron microprobe analysis; all iron as FeO; Ba, K, REE, Al, and Ti are below detection limits. Numerals under the samples are the number of analyses; c, m, r — core, middle, and rim.

*** — Crystallite in fayalite, # — crystallite in magnetite.**

Table 9

Chemical Composition (wt.%) of Leucite and K-Feldspar from Parabasalts of the Southern Urals

Component	Leucite							Component	K-Ba-feldspar									
	parabasalt dropstone			massive parabasalt		veined parabasalt			massive parabasalt						veined parabasalt			
	Sample 0107			Sample KR-6		Sample 42-17			Sample KR-5			Sample KR-6			Sample 42-17			
	1	1	2	9	1	5	1		1	2	3	1	4	3	3	1	4	2
SiO_2	54.01	55.05	55.40	55.75	55.88	55.49	55.59	SiO_2	64.16	62.08	61.84	64.49	63.46	61.32	62.10	59.92	61.38	57.74
TiO_2	0.01	0.04	0.02	0.04	0.06	0.01	0.01	TiO_2	0.13	0.16	0.18	0.16	0.12	0.14	0.00	0.00	0.25	0.19
Al_2O_3	22.74	22.72	22.69	22.73	22.75	22.71	22.55	Al_2O_3	18.43	20.13	19.19	18.64	19.38	19.26	19.30	20.31	18.76	19.91
Fe_2O_3	1.98	0.90	0.56	0.34	0.13	0.29	0.76	Fe_2O_3	0.37	0.40	0.37	0.16	0.30	0.45	0.46	0.42	0.49	0.58
MnO	0.00	0.00	0.00	0.01	0.00	0.01	0.02	MnO	0.00	0.01	0.01	0.01	0.01	0.01	0.00	0.00	0.00	0.01
MgO	0.03	0.02	0.02	0.00	0.00	0.02	0.03	MgO	0.01	0.01	0.01	0.02	0.01	0.02	0.02	0.01	0.01	0.02
CaO	0.05	0.07	0.10	0.01	0.00	0.01	0.01	CaO	0.28	2.03	0.88	0.33	0.94	0.51	0.71	1.72	0.24	0.69
BaO	0.44	0.44	0.49	0.00	0.00	0.03	0.07	BaO	0.63	1.14	1.95	0.01	0.63	3.26	2.24	3.80	3.57	7.54
SrO						0.02	0.05	SrO							0.08	0.26		0.27
Na_2O	0.26	0.24	0.24	0.09	0.09	0.23	0.06	Na_2O	0.47	0.57	0.56	0.45	0.49	0.89	0.59	0.60	0.34	0.08
K_2O	20.72	20.65	20.86	20.78	21.25	20.78	21.01	K_2O	15.54	13.88	14.19	15.96	14.96	13.75	14.53	13.08	14.96	12.87
Total	100.24	100.13	100.35	99.76	100.16	99.59	100.17	Total	100.01	100.39	99.18	100.23	100.29	99.61	100.03	100.12	100.01	99.90
Formula calculated for 6 oxygens								*Formula calculated for 8 oxygens*										
Si	1.973	2.001	2.009	2.021	2.021	2.018	2.015	Si	2.977	2.880	2.917	2.976	2.935	2.904	2.915	2.842	2.916	2.820
Ti	0.000	0.001	0.000	0.001	0.001	0.000	0.000	Ti	0.005	0.005	0.006	0.006	0.004	0.005	0.000	0.000	0.009	0.007
Al	0.979	0.974	0.970	0.971	0.970	0.973	0.964	Al	1.008	1.101	1.067	1.014	1.056	1.075	1.068	1.136	1.050	1.146
Fe^{3+}	0.055	0.025	0.015	0.009	0.004	0.008	0.021	Fe^{3+}	0.013	0.014	0.013	0.005	0.011	0.016	0.016	0.015	0.017	0.021
Mn	0.000	0.000	0.000	0.000	0.000	0.000	0.001	Mn	0.000	0.000	0.000	0.000	0.000	0.000	0.000	0.000	0.000	0.000
Mg	0.002	0.001	0.001	0.000	0.000	0.001	0.002	Mg	0.000	0.001	0.001	0.001	0.001	0.001	0.001	0.001	0.001	0.002
Ca	0.002	0.003	0.004	0.000	0.000	0.000	0.000	Ca	0.014	0.101	0.044	0.016	0.046	0.026	0.036	0.087	0.012	0.036
Ba	0.006	0.006	0.007	0.000	0.000	0.000	0.001	Ba	0.011	0.021	0.036	0.000	0.011	0.060	0.041	0.071	0.066	0.144
Sr						0.001	0.001	Sr							0.002	0.007		0.008
Na	0.018	0.017	0.017	0.006	0.006	0.016	0.004	Na	0.042	0.051	0.051	0.040	0.044	0.082	0.053	0.055	0.032	0.007
K	0.966	0.958	0.965	0.961	0.981	0.964	0.972	K	0.920	0.821	0.854	0.940	0.883	0.831	0.870	0.792	0.907	0.802
Total of cations	4.002	3.986	3.988	3.971	3.984	3.982	3.980	Total of cations	4.989	4.994	4.989	4.999	4.991	5.002	5.004	5.006	5.010	4.994
End-members								*End-members*										
$KAlSi_2O_6$	92.0	94.9	95.7	98.3	99.0	97.4	97.1	$KAlSi_3O_8$	92.0	81.6	85.5	93.7	88.7	81.9	85.4	77.2	87.6	78.8
$KFeSi_2O_6$*	5.3	2.5	1.6	0.9	0.4	0.9	2.3	$KFeSi_3O_8$*	1.2	1.0	1.2	0.6	0.9	1.3	1.4	1.0	1.6	1.6
$NaAlSi_2O_6$	1.9	1.7	1.7	0.6	0.6	1.6	0.4	$NaAlSi_3O_8$	4.2	5.1	5.2	4.0	4.5	8.2	5.3	5.4	3.1	0.7
$CaAl_2SiO_6$	0.2	0.3	0.4	0.0	0.0	0.0	0.0	$CaAl_2Si_2O_8$	1.4	10.1	4.5	1.6	4.7	2.6	3.6	8.6	1.2	3.6
$(Ba,Sr)Al_2SiO_6$	0.6	0.6	0.7	0.0	0.0	0.1	0.2	$(Ba,Sr)Al_2Si_2O_8$	1.2	2.1	3.7	0.0	1.2	6.1	4.3	7.7	6.5	15.2

***With consideration of magnesian end-members ($KMg_{0.5}Si_{2.5}O_6$ and $KMg_{0.5}Si_{3.5}O_8$), numerals under the samples are the number of analyses.**

Table 10

Chemical Composition (wt.%) of Sulfides in Veined Parabasalt (Sample 42-17)

Mineral	Fe	Ni	Cu	Zn	Ca	S	Total	S	Me/S	Fe/Cu
								at.%		
Pyrrhotite	60.17	0.01	0.00	0.00	0.06	39.47	99.71	53.3	0.876	
	60.51	0.02	0.00	0.00	0.10	39.46	100.09	53.1	0.883	
	60.53	0.08	0.00	0.03	0.11	39.64	100.38	53.2	0.880	
	60.20	0.05	0.00	0.03	0.01	39.29	99.58	53.2	0.881	
	60.72	0.03	0.00	0.00	0.02	39.12	99.89	52.9	0.892	
	60.09	0.09	0.00	0.03	0.06	39.61	99.87	53.4	0.874	
	60.19	0.10	0.02	0.00	0.02	39.20	99.54	53.1	0.884	
	60.12	0.60	0.01	0.02	0.01	39.24	100.00	53.0	0.888	
	60.70	0.02	0.00	0.00	0.02	39.19	99.93	52.9	0.890	
	60.47	0.01	0.00	0.00	0.07	39.52	100.06	53.2	0.880	
	60.68	0.01	0.00	0.00	0.08	39.19	99.95	52.9	0.891	
	60.46	0.06	0.01	0.01	0.04	39.52	100.09	53.2	0.880	
	60.79	0.01	0.00	0.01	0.03	39.11	99.95	52.8	0.893	
	58.02	2.15	0.00	0.02	0.02	39.40	99.61*	53.3	0.876	
Pyrite	49.06	0.05	0.15	0.01	0.02	50.50	99.79	64.1	0.560	
	47.83	0.03	0.35	0.00	0.03	51.69	99.93	65.1	0.535	
	48.56	0.08	0.26	0.00	0.06	50.93	99.90	64.4	0.552	
	48.81	0.16	0.30	0.00	0.08	50.46	99.80	64.1	0.561	
	48.97	0.03	0.09	0.00	0.06	50.72	99.87	64.2	0.556	
	49.55	0.04	0.07	0.00	0.03	50.37	100.06	63.8	0.566	
	49.16	0.01	0.25	0.01	0.03	50.78	100.24	64.1	0.559	
Chalcopyrite	34.44	0.05	30.63	0.18	0.01	34.65	99.96	49.5	1.020	1.28
	34.19	0.00	30.45	0.16	0.01	34.88	99.69	49.9	1.006	1.28
	35.66	0.03	28.65	0.69	0.00	34.84	99.87	49.7	1.013	1.42

***Sulfide globule in glass at the contact of parabasalt with annealed mudstone.**

composition (wt.%) is as follows: SiO_2 – 44.18, TiO_2 – 0.06, Al_2O_3 – 31.41, FeO – 0.91, MgO – 0.07, CaO – 1.51, BaO – 0.05, Na_2O – 13.00, K_2O – 8.89. Earlier a sodium phase (nepheline or carnegieite) was qualitatively identified in basic paralavas from Wyoming only [4].

Potassic feldspar is a late interstitial phase, which in massive parabasalts is brown, opaque or weakly transparent and often looks isotropic. Occasionally zonal anorthite crystals are surrounded by a K-feldspar rim. In veined parabasalts it is colorless and forms xenomorphic grains in interstices. The contents of BaO vary from 0.1 to 7.5 wt.% (see Table 9). Potassic feldspars with high BaO concentrations also contain SrO (to 0.3 wt.%); other admixtures (wt.%) are: Fe_2O_3 – 0.2–0.6, CaO – 0.3–2.0, Na_2O – 0.1–0.6.

Sulfides are typical ore phases in parabasalts of the Southern Urals, they form segregations of various shapes in interstices and are closely associated with titanomagnetite. Veined varieties sometimes contain sulfide globules (measuring to 5–10 μm) in glass and later minerals (fayalite, kirschsteinite, and hedenbergite). In large (to 100–150 μm) sulfide segregations the major mineral is pyrrhotite, the rims occasionally contain pyrite, chalcopyrite, and, possibly, pentlandite (see Fig. 1, *b*). In sulfur content pyrrhotites vary from Fe_9S_{10} (hexapyrrhotite, Me/S = 0.9 (at.%) to Fe_7S_8 (clinopyrrhotite, Me/S = 0.875), but the majority of compositions are close to Fe_8S_9 (Me/S = 0.889) (Table 10). Concentrations of nickel are usually low (Ni < 0.10 wt.%), but some pyrrhotites of globules might contain to 0.6–2.2 wt.% Ni. In chalcopyrite, iron prevails over copper (Fe/Cu = 1.28–1.42 at.%), the amount of Zn varies from 0.15 to 0.7 wt.%, and the concentration of Ni is no

higher than 0.05 wt.%. The composition of pyrite differs from the ideal one in higher concentration of Fe (Me/S = 0.53–0.57 at.%). According to experimental data [34, 35], the pyrrhotite + pyrite + chalcopyrite association is stable at 739–743 °C.

Ilmenite is fairly distinctly identified only in veined parabasalts. Typically it forms single laths in acidic glass and, less often, large lamellae in titanomagnetite at the contact of parabasalt with annealed mudstone (Table 7). Its composition is characterized by increased concentrations of the following end-members (mol.%): $FeTiO_3$ – 80.6–81.2, $MgTiO_3$ – 5.6–5.7, Fe_2O_3 – 10.5–11.1. The amounts of MnO and Al_2O_3 are no more than 1 wt.%.

Polymorphs of SiO_2 are scarce in parabasalts and occur at the contacts with vitrified mudstones, which occasionally contain fused grains of detrital quartz. Tridymite and cristobalite, identified by X-ray powder diffraction, refer to newly formed minerals [8]. Tridymite forms granular aggregates (to 100 μm in size) in interstices between plagioclase and pigeonite. Its chemical composition is (wt.%): SiO_2 – 98.6, TiO_2 – 0.25, Al_2O_3 – 0.57, FeO – 0.12, MnO – 0.01, CaO – 0.24, Na_2O – 0.02, K_2O – 0.20.

Schungite-like material occurs in massive parabasalts as xenoliths to 2 cm in size. Native iron was also identified here by X-ray powder diffraction.

Two types of glasses are common to parabasalts: K-acidic and Fe-basic. Acidic glasses are predominantly concentrated in veined parabasalts, whereas basic glasses in dropstones.

Basic high-iron glasses are opaque and finely devitrified, they occur mainly in mesostasis of parabasalt dropstone, are very scarce in massive varieties, and exist as melt inclusions in leucocratic minerals of veined parabasalts (plagioclase and leucite). They widely vary in composition (wt.%): FeO to 46, SiO_2 = 28–35, and Al_2O_3 = 2.5–5.5 (Table 11). Interstitial glasses of parabasalt dropstone are close to fayalite, and glasses in leucocratic minerals of veined parabasalts – to kirschsteinite and high-calcium fayalite.

Acidic potassic glasses occur in interstices between crystals of rock-forming silicates of veined parabasalts and, seldom, as melt inclusions in fayalite of veined and massive varieties. They are dark-brown, isotropic, and, unlike crystal phases, "burn" under microprobe beam owing to intense evaporation of potassium and volatiles. The overwhelming majority of them correspond to a narrow range of compositions (wt.%): SiO_2 – 72–78, Al_2O_3 – 10–14, K_2O – 5–8, FeO – 1–3 (see Table 11). Separate sites of the glasses have high concentrations of SiO_2 (to 80 wt.%) or are similar to orthoclase (SiO_2 <69 wt.%). Unlike later interstitial K-feldspars, the glasses constantly contain phosphorus (P_2O_5 – 0.2–1.7 wt.%) and, occasionally, traces of chlorine and fluorine – to 0.1 wt.% (at their detection limits of 0.01 and 0.08 wt.%, respectively). Normative compositions of acidic glasses from parabasalts are rather accurately reflected on the $CaAl_2Si_2O_8$–$KAlSi_3O_8$–SiO_2 diagram (Fig. 4). They have nearly the same chemical composition as the glasses from the fine-grained chilled zone at the contact with mudstones, except lower concentrations of TiO_2.

Only once coexisting acidic and basic glasses were found in mesostasis of massive parabasalt (sample KR-6) (see Table 11). Earlier, similar phenomena were recognized in melt inclusions in minerals and in groundmass of low-magnesium basalts of the Moon and also in plagioclase-hosted inclusions from lavas of Karymskii volcano (Kamchatka) [36, 37]. These phenomena are explained in terms of liquid immiscibility – separation of initial melt into two silicate liquids (K-acidic and Fe-basic).

DISCUSSION

The majority of silicate melts appear at long-term and constant temperatures higher than 1000 °C. That is why in the course of burning of coal spoil heaps considerable accumulations of parabasalts form rarely. Such conditions were realized during the burning of the largest spoil heaps in the Chelyabinsk brown-coal basin [7–10, 18]. Their huge sizes in combination with high porosity, which favored active gas blow through heaps, and significant amounts of coal material (about 20%) allowed generation and accumulation of heat energy required for silicate melts to appear. The overlying heated rocks acted as a heat isolator ensuring slow crystallization of melts.

Direct observations of the relationships of rock fragments in the zones of melting inside spoil heaps allowed Chesnokov and Shcherbakova [7] to suggest that the source of melt was a finely crushed fusible mixture of mudstones (Si, Al, K, Ti), clay-carbonate sediments (Al, Ca, Mg), and siderites (Fe, Mn, P) in the presence of coal material (C, S, N).

Their combined melting in high-temperature zones of spoil heaps under reductive conditions and at pressure close to the atmospheric one resulted in hybrid melts whose compositions appeared to be shifted (compared to terrestrial basic rocks) toward a considerable enrichment in Fe, Ca, Al, and Ti and depletion

Table 11

Chemical Composition (wt.%) of Interstitial Glasses and Inclusion Glasses in Parabasalt Minerals

Component	Parabasalt dropstone		Massive parabasalt		Veined parabasalt																			
	Sample 0107		Sample KR-6		Sample 42-17																		Sample 063-45	
	interst. glass		interst. glass*		inclusions in plagioclase		inclusions in leucite			inclusions in fayalite					interstitial glass								interstitial glass	
SiO_2	31.96	34.00	31.24	73.36	35.00	34.17	33.93	32.12	31.60	68.73	69.72	72.11	78.50	79.17	72.93	73.64	74.55	75.51	77.08	77.47	77.97	80.24	74.93	76.03	78.03
TiO_2	0.05	0.09	6.72	0.76	1.39	0.94	0.60	1.30	0.56	0.37	0.49	0.55	0.25	0.42	0.21	0.22	0.35	0.28	0.20	0.81	0.37	0.36	0.45	0.41	0.40
Al_2O_3	2.46	3.05	3.42	12.66	3.96	5.46	2.99	5.52	2.66	12.88	10.59	12.04	10.70	11.64	14.48	12.71	12.84	10.16	12.18	10.68	10.58	10.96	11.34	12.37	13.42
FeO	46.60	46.33	28.05	3.06	28.11	30.29	36.69	38.00	46.22	2.89	4.56	3.22	1.48	1.57	1.08	1.20	1.18	1.60	1.56	1.57	0.49	0.62	1.46	0.78	0.96
MnO	1.29	1.28	0.61	0.05	0.45	0.68	0.72	0.67	1.17	0.00	0.22	0.13	0.00	0.01	0.00	0.00	0.00	0.04	0.00	0.00	0.01	0.00	0.07	0.04	0.04
MgO	11.09	9.79	1.55	0.09	6.21	3.82	1.48	3.02	1.34	0.49	0.30	0.18	0.04	0.02	0.01	0.01	0.01	0.22	0.01	0.04	0.02	0.03	0.24	0.11	0.05
CaO	3.44	2.51	17.38	0.96	17.64	17.45	15.62	14.33	10.11	1.16	1.59	1.94	0.60	0.54	0.41	0.40	0.39	1.76	0.53	2.03	1.94	4.82	1.23	0.64	0.36
BaO			0.00	0.06	0.15	0.02	0.08	0.11	0.04	0.37	0.34	0.32	0.59	0.26	1.00	0.14	0.12	0.96	0.19	0.20	2.39	0.91	0.61	0.34	0.03
SrO					0.01	0.04	0.01	0.06	0.07	0.00	0.00	0.00	0.00	0.00						0.00					
Na_2O	0.12	0.11	0.14	0.40	0.29	0.28	0.29	0.18	0.17	0.71	0.10	0.05	0.25	0.15	0.63	0.55	0.58	0.08	0.62	0.07	0.14	0.33	0.31	0.23	0.07
K_2O	0.11	2.12	1.10	7.92	1.31	1.09	0.55	0.25	0.53	8.89	5.98	5.26	7.17	5.17	6.73	8.31	8.04	6.94	5.87	5.10	5.13	1.57	7.26	8.25	3.70
P_2O_5	0.52	0.13	8.60	0.26	1.24	1.66	2.80	2.12	3.27	0.15	0.16	0.25	0.20	0.14	0.56	1.60	1.73		0.62	0.18					
F															0.01	0.02	0.03		0.01						
Cl			0.00	0.00			0.05	0.02	0.01					0.00	0.11	0.10	0.09		0.08						
SO_3			0.83	0.04			0.70	1.20	0.94					0.01											
Total	97.64	99.41	99.64	99.62	95.75	95.90	96.51	98.90	98.70	96.64	94.05	96.05	99.78	99.10	98.16	98.90	99.91	97.57	98.95	98.15	99.14	99.86	97.91	99.18	97.09

Note. Interstitial high-Fe glass in parabasalts is finely devitrified. Inclusions in plagioclase and leucite of veined parabasalt consist of finely devitrified aggregate + gas.

*** Coexisting glasses in interstices of massive parabasalt. $ is the phase composition of inclusion in fayalite: glass + K-feldspar + magnetite + gas; the other inclusions are glass + gas.**

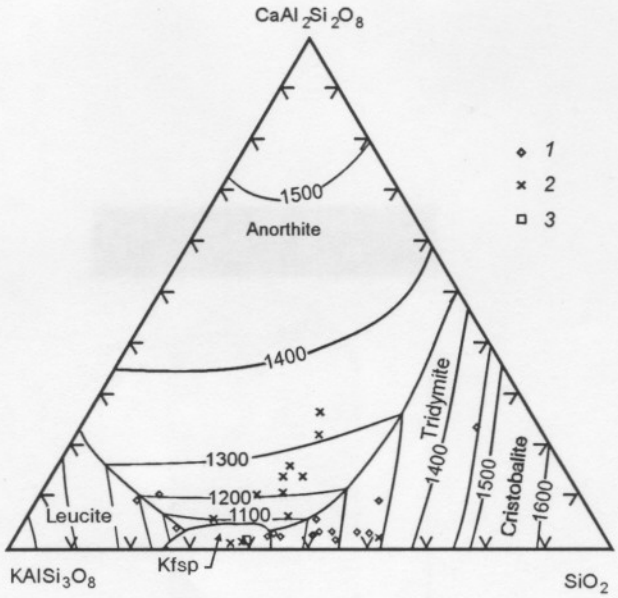

Fig. 4. Normative $CaAl_2Si_2O_8$–$KAlSi_3O_8$–SiO_2 composition diagram of acidic glasses from technogenic veined parabasalts from the Southern Urals and natural paralavas. The diagram is reproduced from [4]. Glasses: *1* – from parabasalts, *2* – from paralavas of Wyoming [4], *3* – from paralavas of Eastern Kazakhstan [6].

in K, Na, Si, and H_2O. The place of traditional melt-forming components (alkalies + water) in this case was occupied by Fe^{2+}, P, F, and Cl [10].

The appearance of melts in spoil heaps of the Southern Urals was preceded by amorphization of clays and micas, decomposition of Ca-Mg-carbonates, and dissociation of siderite. We have established that thermal destruction of phyllosilicates in mudstones occurs at the stage of yellow fused rocks (T = 600–700 °C) and is accompanied by intense dehydration and nearly complete burning-out of sodium [8–10]. Further increase in annealing temperature results in acidic K-Al-glass. The products of thermal dissociation of carbonates – lime (or later portlandite), periclase, and black foam of hematite-magnetite composition – are ordinary components of red fused rocks (T = 700–800 °C). Evidence for the participation of the above-mentioned compounds and ferrites in the formation of parabasalt melt in spoil heaps was found within the above reaction zones at the contacts of parabasalts with fragments of petrified wood and annealed mudstones, where all phases (except pure FeO) were diagnosed, earlier postulated as melt-forming by analogy with agglomerates [24]. These facts suggest that the mechanisms of formation of synthetic (metallurgy), technogenic (spoil heaps), and natural (fused rocks of Eastern Kazakhstan) low-temperature iron-silicate melts are identical.

Preliminary thermometric studies of melt inclusions in the early minerals of parabasalts (plagioclase, clinopyroxene) show that crystallization of these rocks started at temperatures higher than 1200 °C. The melting point of metastasis was also determined experimentally and is approximately 1000 °C. The pressure at which melts originated and crystallized is close to the atmospheric one.

The presence of schungite, oldhamite (CaS), pyrrhotite, and native iron in technogenic rocks and regular coexistence of fayalite with titanomagnetite indicates that the partial oxygen pressure does not exceed the values of the QFM buffer. According to calculated data [38, 39], oxygen fugacity at the initial stages of parabasalt crystallization was $10^{-8.3–9.4}$ at 1300–1200 °C (liquidus) and at the final stages – $10^{-12.2}$ at 1000 °C (magnetite-ilmenite association). The incorporation of phosphorus into the structures of olivine and kirschsteinite is also indirect evidence of low oxygen fugacity [22].

According to petrographic relationships of minerals, the approximate order of formation of phases in veined parabasalts is as follows: Al-spinel → plagioclase → Mg-Fe-clinopyroxene → Mg-Fe-olivine → leucite → titanomagnetite, pyrrhotite, apatite → fayalite, kirschsteinite, hedenbergite → K-feldspar, ilmenite → acidic K-Al-glass. In the case of parabasalt dropstone, the phases formed in the following order: Al-spinel → plagioclase → Mg-Fe-clinopyroxene → Mg-Fe-olivine → leucite → titanomagnetite, pyrrhotite, apatite →

(fayalite, kirschsteinite) → basic Fe-rich glass. The crystallization sequence of phases in massive parabasalt is nearly the same as in veined parabasalts, but the role of later Ca-Fe-minerals (hedenbergite, kirschsteinite) is insignificant.

During the crystallization of early minerals (Al-spinel, anorthite, Mg-Fe-clinopyroxene, Mg-Fe-olivine, leucite), the initial parabasalt melt was gradually enriched in P, Mn, Fe, and Ti depleted in Si, Al, and, negligibly, Ca. All this favored formation of later phases with low Si content and high Fe concentration (magnetite, pyrrhotite, fayalite, hedenbergite, apatite, and kirschsteinite). The result of crystallization of the youngest high-Fe association is that the residual melt was enriched in Si, Al, Ba, and alkalies and depleted in mafic components. This melt (prior to its solidification) was the source for small amounts of Ba-K-feldspar and ilmenite. Thus, during crystallization, the composition of parabasalt melt gradually evolved from Fe-rich basalt (1250–1200 °C) to rhyolite (1100–1000 °C). Liquid immiscibility phenomena (separation of the melt into K-acidic and Fe-basic silicate liquids) during the formation of parabasalts were extremely rare. It is possible that, during crystallization, the parabasalt melt could have actively reacted with xenoliths of annealed mudstones (veined parabasalts). This process might also have favored its enrichment in SiO_2 at the final crystallization stages.

The systems studied are in essence anhydrous. It was proved that fluid components involved in petrogenesis of parabasalts are F, Cl, P, and S; the role of CO, CO_2, and various hydrocarbons is also significant [7, 32]. As a result, basic rock associations lack hydrous minerals where the positions of (OH)-groups are occupied by F or Cl. A shining example is apatites. Low water concentrations in fluid and residual melt inhibited retrograde alteration of high-temperatures associations.

We think that the specific chemical composition of some phases in the studied rocks is explained, firstly, by the influence of fused substratum with high contents of Fe, Ca, and Al (which, in fact, turns these rocks into fluxed iron-silicate systems) and, secondly, by the specific cooling regime. At the same time, technogenic parabasalts possess all typical properties of shallow-depth basic rocks. These are, for example, structure-textural features, the range of rock-forming and accessory minerals, their ratios, and crystallization sequence of phases. The reductive conditions under which melts crystallized are responsible for the fact that the closest analogs of the studied rocks are lunar low-magnesium basalts and dolerites cooled in a vacuum [13, 14].

We express our sincere thanks to B. V. Chesnokov (Institute of Mineralogy, Miass) for parabasalt samples, to N. V. Vladykin (Institute of Geochemistry, Irkutsk) for determining the trace-element composition of the rocks, and to D. V. Kuz'min (Institute of Mineralogy and Petrography, Novosibirsk) for thermometric studies of melt inclusions.

The work was finacially supported by grant 98-05-65257 from the Russian Foundation for Basic Research.

REFERENCES

[1] V. Venkatesh, *Amer. Miner.*, vol. 37, p. 831, 1952.

[2] A. Miyashiro, T. Iliyama. M. Yamasaki, and T. Miyashiro, *Amer. J. Sci.*, vol. 253, no. 4, p. 185, 1955.

[3] F. F. Foit, R. L. Hooper, and P. E. Rosenberg, *Amer. Miner.*, vol. 72, p. 137, 1987.

[4] M. A. Cosca, E. J. Essene, J. W. Geissman, et al., *Amer. Miner.*, vol. 74, p. 85, 1989.

[5] Y. K. Bentor, M. Kastner, I. Perlman, and Y. Yellin, *Geochim. Cosmochim. Acta*, vol. 45, p. 2229, 1981.

[6] I. A. Kalugin, G. A. Tret'yakov, and V. A. Bobrov, *Iron-ore basalts in fused rocks of Eastern Kazakhstan* [in Russian], Novosibirsk, 1991.

[7] B. V. Chesnokov and E. P. Shcherbakova, *The mineralogy of burned heaps in the Chelyabinsk coal basin* [in Russian], Moscow, 1991.

[8] E. V. Sokol, N. I. Volkova, and G. G. Lepezin, *Eur. J. Miner.*, vol. 10, p. 1003, 1998.

[9] E. V. Sokol, E. N. Nigmatulina, and A. E. Frenkel, *Ural'skii Mineralogicheskii Sbornik*, no. 10, p. 15, 1999.

[10] E. V. Sokol, E. N. Nigmatulina, and A. E. Frenkel', *ibid.*, p. 27.

[11] V. V. Ryabov, A. L. Pavlov, and G. G. Lopatin, *Native iron of Siberian traps* [in Russian], Novosibirsk, 1985.

[12] F. Sh. Kutyev and V. N. Sharapov, *Petrogenesis beneath volcanoes* [in Russian], 1979.

[13] *Magmatism of the Earth and the Moon: experience of a comparative analysis* [in Russian], Moscow, 1990.

[14] E. J. Essene, A. E. Ringwood, and N. G. Ware, in: *Proceedings of the Apollo 11 lunar science conference, vol. 1 (Mineralogy and petrology)*, p. 385, 1970.

[15] C. Savelli, *Contr. Miner. Petrol.*, vol. 16, p. 328, 1967.

[16] A. Cundari, *Contr. Miner. Petrol.*, vol. 70, p. 9, 1979.

[17] P. M. Holm, S. Lou, and E. Nielsen, *Contr. Miner. Petrol.*, vol. 80, p. 367, 1982.

[18] B. V. Chesnokov, *Ural'skii Mineralogicheskii Sbornik*, no. 7, p. 5, 1997.

[19] N. Morimoto, J. Fabries, A. K. Ferguson, et al., *Amer. Miner.*, vol. 73, p. 1123, 1988.

[20] P. R. Buseck and J. Clark, *Miner. Mag.*, vol. 48, no. 347, p. 229, 1984.

[21] C. A. Goodrich, *Geochim. Cosmochim. Acta*, vol. 48, no. 5, p. 1115, 1984.

[22] S. O. Agrell, N. R. Charnley, and G. A. Chinner, *Miner. Mag.*, vol. 62, no. 2, p. 265, 1998.

[23] T. Kanazawa, *Inorganic phosphate minerals*, Tokyo, 1989.

[24] T. Ya. Malysheva, *Iron-ore raw material: heat-treatment hardening* [in Russian], Moscow, 1988.

[25] N. V. Chalapanthi Rao, S. J. B. Reed, D. M. Pyle, and P. D. Beattie, *Miner. Mag.*, vol. 60, p. 513, 1996.

[26] T. Mikouchi, H. Takeda, M. Miyamoto, et al., *Amer. Miner.*, vol. 80, p. 585, 1995.

[27] L. Folco and M. Mellini, *Eur. J. Miner.*, vol. 9, p. 969, 1997.

[28] A. G. Anshits, E. N. Voskresenskaya, E. V. Kondratenko, et al., *Catalysis Today*, vol. 42, no. 2, p. 197, 1998.

[29] Th. G. Sahama and K. Hytonen, *Miner. Mag.*, vol. 31, no. 239, p. 698, 1957.

[30] Th. G. Sahama and K. Hytonen, *Amer. Miner.*, vol. 43, nos. 9–10, p. 862, 1958.

[31] A. A. Konev and V. S. Samoilov, *Contact metamorphism and metasomatism in the aureole of the Tazheran alkaline intrusion* [in Russian], 1974.

[32] B. V. Chesnokov, *Dokl. RAN*, vol. 343, no. 1, p. 94, 1995.

[33] Y. Liu and P. Comodi, *Miner. Mag.*, vol. 57, p. 709, 1993.

[34] E. H. Roseboom and G. Kullerud, *Carnegie Inst. Wash. Year Book 1957*, p. 222, 1958.

[35] G. Kullerud, *Carnegie Inst. Wash. Year Book 1962*, p. 175, 1963.

[36] E. Roedder and P. W. Weiblen, in: *Proceedings of the Apollo 11 lunar science conference, vol. 1 (Mineralogy and petrology)*, p. 801, 1970.

[37] N. F. Krasov and R. Clocchiatti, *Dokl. AN SSSR*, vol. 248, no. 1, p. 201, 1979.

[38] R. O. Sack, I. S. E. Carmichael, M. Rivers, and M. S. Chiorso, *Contr. Miner. Petrol.*, vol. 75, p. 369, 1980.

[39] D. J. Andersen, D. H. Lindsley, and P. M. Davidson, *Computers and Geosciences*, vol. 19, no. 9, p. 1333, 1993.

Recommended by V. A. Kutolin Received 21 July 1998